RESEARCH MEMORANDUM

WIND-TUNNEL INVESTIGATION OF THE AERODYNAMIC AND STRUCTURAL DEFLECTION CHARACTERISTICS OF THE GOODYEAR INFLATOPLANE

By Bennie W. Cocke, Jr.

Langley Aeronautical Laboratory
Langley Field, Va.

NATIONAL ADVISORY COMMITTEE
FOR AERONAUTICS

WASHINGTON

September 10, 1958

NACA RM L58E09

NATIONAL ADVISORY COMMITTEE FOR AERONAUTICS

RESEARCH MEMORANDUM

WIND-TUNNEL INVESTIGATION OF THE AERODYNAMIC AND STRUCTURAL DEFLECTION CHARACTERISTICS OF THE GOODYEAR INFLATOPLANE[1]

By Bennie W. Cocke, Jr.

SUMMARY

An investigation has been conducted in the Langley full-scale tunnel to determine the aerodynamic and structural deflection characteristics of the Goodyear Inflatoplane over a range of test velocities from minimum stall speed up to speeds giving load factors for wing buckling. Tests were conducted over a range of speeds from approximately 41 to 70 mph with wing-guy-cable loads, wing-distortion photographs, and aerodynamic-force data recorded at each speed for a full range of angle of attack.

The airplane was longitudinally stable and had adequate pitch and roll control and normal stall characteristics at the lower speeds giving maximum load factors between 1 and 1.5. However, as speed was increased, aeroelastic effects associated with wing twist produced an increase in lift-curve slope and loss of stability near the stall. For speeds up to 65 mph, which produced a load factor of approximately 2, the maximum wing load was limited by stall with moderate wing deflections. However, at a speed just over 70 mph and at an attitude producing a load factor just over 2, a column-type buckling occurred on the inboard wing panel with the inboard wing section folding up and contacting the engine mounted above the wing. Additional tests were made with modifications to the wing-guy-cable system which reduced the aeroelastic effects on the aerodynamic characteristics and allowed load factors up to approximately 2.5 before a tendency for wing buckling occurred.

---

[1]The information presented herein was previously given limited distribution.

INTRODUCTION

The need for a means of rescue or escape for fliers downed in enemy territory has prompted the Military Services to consider a number of possible rescue concepts. One scheme considered would utilize a small lightweight airplane made from inflatable structure which when deflated could be completely contained in a small lightweight package and parachuted to a downed man for self-rescue at the most opportune moment. This idea has been developed under contract by the Office of Naval Research to the point of successful flight demonstration of a single-place prototype model which can be deflated and packaged in a size and weight which can be handled by one man.

As the pneumatic structure used in this airplane is novel and does not lend itself to existing structural theory, the prototype airplane was tested in the Langley full-scale tunnel to obtain data on its characteristics under various aerodynamic loadings up to wing failure to provide data for correlation with existing theory developed from static-load tests.

This report presents the results of the wind-tunnel tests, during which the aerodynamic characteristics and control effectiveness were obtained in addition to wing-guy-cable loadings and wing-deflection records for a range of wind velocities from approximately 36 to 70 mph. The characteristics of the configuration were also determined for a range of reduced inflation pressures simulating leakage due to battle damage or compressor malfunction.

SYMBOLS

C_L lift coefficient, $\frac{\text{Lift}}{qS}$

C_D drag coefficient, $\frac{\text{Drag}}{qS}$

C_m pitching-moment coefficient, $\frac{\text{Pitching moment}}{qS\bar{c}}$

C_n yawing-moment coefficient, $\frac{\text{Yawing moment}}{qSb}$

C_l rolling-moment coefficient, $\frac{\text{Rolling moment}}{qSb}$

q	free-stream dynamic pressure, lb/sq ft
S	wing area, sq ft
$\bar{c}$	mean aerodynamic chord, ft
b	wing span, ft
α	angle of attack (angle between relative wind and fuselage water line 50), deg
V	stream velocity, mph
P_f	fuselage inflation pressure, lb/sq in.
P_w	wing inflation pressure, lb/sq in.
δ_e	elevator deflection angle, positive when trailing edge deflected down, deg
δ_a	aileron deflection angle, positive when trailing edge deflected down, deg
δ_s	control stick deflection angle, deg

Subscripts:

L	left
R	right
av	average

AIRPLANE AND APPARATUS

The Goodyear Inflatoplane used in this program is composed of pneumatic structure throughout with exceptions of the engine, engine mount, landing gear, and miscellaneous short control members. All inflatable components are interconnected in a manner allowing a small compressor on the 40-hp air-cooled engine to maintain a constant regulated pressure in the system even with moderate leakage. The wing and tail surfaces are woven in a manner such that the upper and lower airfoil surfaces are connected internally by nylon drop threads varying in length to produce the approximate shape control desired in any

surface when inflated. A circular fuselage is utilized with a fuel bag internally mounted and the cockpit section is constructed using sections of air mat material 2 inches thick. Design gross weight of the airplane is 550 pounds with 120 pounds of fuel and 240 pounds payload.

Each wing panel is restrained by two guy cables on the upper and lower surfaces with the two upper cables anchored to the engine pylon and the two lower cables anchored to the landing gear. Both upper and lower cables attach to patches bonded to the wing surface approximately $0.57\frac{b}{2}$ out from the center line. A general layout with pertinent geometric data is shown in figure 1 and a photograph of the airplane is presented in figure 2. The propeller was removed for this load program primarily for safety considerations.

The airplane was mounted for tests on the conventional six-component mechanical balance as shown in figure 3. A special yoke (fig. 3(b)) was utilized to mount the airplane so that strut restraining loads were transmitted to the fuselage through strap attachments located beneath the wing quarter-chord point thus leaving the wings free to deflect while being restrained only by the normal wing-fuselage and guy-cable attachments as in flight. The tail strut was attached to a saddle strapped to the rear of the fuselage (fig. 3(c)) and was connected by cables to the front support yoke thus preventing longitudinal tail strut loads from being transmitted into the fuselage.

An actuator system was installed in the cockpit to allow remote operation of the elevators and ailerons which were equipped with control-position transmitters located on the respective surfaces to record the position settings of each control. Control-position transmitters were placed on both the right and left side of the elevator surface to give indication of the amount of twist occurring under load since the elevator was actuated by a single horn. Strain-gage units were installed in all wing guy cables for cable load evaluation, and cameras were set up to record the deflection of the left wing panel under the various loading conditions. The left wing was chosen for photographic study as the contours and wing geometry of the panel were more uniform than those of the right panel.

TESTS

The objective of this program was to determine the aerodynamic and wing deflection characteristics of the Inflatoplane under various loading conditions. Tests were conducted at various airspeeds ranging from approximately 36 to 71 mph with the airplane angle of attack increased by small increments at each airspeed until either wing stall

occurred or the wing buckled. This sequence of tests made with the airplane at normal inflation pressure was repeated for two airplane configurations, namely, the basic original airplane and the airplane with an additional guy cable added to the lower surface of each wing panel to provide additional rigidity. For the configuration with additional guy cables, tests were also made with wing and fuselage pressures reduced for wind speeds near minimum flight speed to determine a safe minimum inflation pressure for maintaining flight. In conjunction with the tests made at normal pressure, aileron and elevator control effectiveness were measured on the original airplane configuration for speeds chosen to represent the minimum and cruise flight regions.

Aerodynamic force and moment data were recorded for each of the runs, and for a representative range of loading conditions, wing-guy-cable loads were recorded along with photographic records of the deflection of the left wing panel. For conditions where wing buckling was reached, motion pictures were used to record the wing motions after collapse.

All data presented in this paper have been corrected for wind-tunnel buoyancy, jet boundary, and stream misalinment. Support-strut tares were not measured since major emphasis was placed on obtaining loads information. All drag results, therefore, include the tare drag of the support system. Pitching-moment data shown are computed for a center of gravity located longitudinally at fuselage station 72.7 and vertically at water line 45.3.

RESULTS AND DISCUSSION

Longitudinal Aerodynamic Characteristics and Wing Buckling Tests

Original airplane configuration.- The results of force measurements (fig. 4) made at various airspeeds for the original Inflatoplane configuration at normal inflation pressure (7 lb/sq in.) showed a marked effect of dynamic pressure on the variations of lift coefficient and pitching moment with airplane attitude. These variations are attributed to aeroelastic effects. At the lower speed $\left(q_{av} = 4 \text{ lb/sq ft}\right)$ which would closely approximate a minimum steady flight speed (approximately 1 g at $C_{L,max}$), the lift curve was linear and the airplane was stable through stall. With increasing speed, an increase in lift-curve slope is apparent and the airplane becomes unstable in the high lift coefficient range representing accelerated flight. For the speeds corresponding to average dynamic pressures of 4, 7, and 10, wing stall was reached at each speed and the value of $C_{L,max}$ obtained was reduced

with increased speed. The $C_{L,max}$ value of 1.0 at q_{av} = 10 lb/sq ft was reached at an α of approximately -2° and gave a load factor slightly less than 2 with moderate wing deflections but no signs of wing failure. With the tunnel speed increased to approximately 71 mph $\left(q_{av} = 12\right)$, a run was made with angle of attack increased by 1° increments, and when an angle of attack of approximately -5° was reached wing buckling occurred suddenly after approximately 30 seconds time had elapsed at this condition. The wing recovered quickly when load was reduced after buckling without any apparent damage, however observation of the wing behavior indicated that if a propeller had been installed and operating the wing would have been destroyed. As it was important to obtain the loadings for this condition, the run was repeated with angle of attack increased by increments of 0.25° up to the -5° attitude of which three load readings were taken prior to collapse. This information showed a steady increase in load with time with the fuselage attitude held constant thus indicating that stretch in the nylon fabric at high loadings was allowing the wing to increase effective attitude with respect to the fuselage. The last recorded load prior to wing buckle for this condition was 1,154 pounds for a load factor slightly in excess of 2.

No apparent damage to the airplane resulted from these first two buckling experiences; therefore, an additional buckling test was programed with more complete motion-picture and still-photographic coverage for study of the rapid motions of the wing during the 2 or 3 cycles of buckling and recovery which the wing went through despite prompt shutdown of the wind tunnel. For this additional photographic run the airplane attitude was slowly increased from -10° to -5° and continuous movie coverage was taken as the wing loaded and buckled. In this sequence the rear wing-guy-cable patch on the lower surface of the left wing tore on the second buckling cycle and the wing contacted the engine and was punctured by the spark plugs and propeller shaft. Photographs showing the wing at the onset of buckling and just after puncture are shown in figure 5. Motion pictures and still photographs of the wing buckling showed a column-type failure inboard approximately midway between the fuselage and wing-guy-cable-attachment points with the wing folding inboard and moving up and in so as to bring the inboard wing sections well into the propeller disk area. Close study of photographs of the buckling runs made prior to the failure of the rear guy-cable patch and wing puncture showed further that the rear guy cable had fouled on the model support system during these runs and actually snubbed the wing in its upward travel, thus probably preventing wing puncture due to contact with engine during the first buckling tests. Initial buckling in all cases occurred on the left wing panel which developed a slightly higher loading than the right panel. This load asymmetry, also indicated by the higher magnitude of the left-wing-guy-cable loads

and by positive airplane rolling moments, was attributed at least in part to negative camber evident in the airfoil sections in the region of the right wing tip.

Airplane with additional wing guy cables.- On the basis of the basic tests it was desirable to modify the wing attachment system to improve the aerodynamic characteristics of the airplane at higher speeds and to improve its load-carrying ability and arrest its motions after wing failure. From studies of the data and photographs it was felt that the aeroelastic effects shown in the data were largely associated with the deflection of the inboard wing sections which resulted in increasing wing incidence with load. This increase was believed to produce an unfavorable downwash at the tail resulting in the loss in stability at higher loadings. As the wing failure was similar to that of an eccentrically loaded column it also was obvious that some additional restraint inboard should give higher load capability, while, at the same time, offering some possibility of improving stability.

During the time used for patching the wing punctures, provisions were made for addition of two new guy cables on the lower surface of each wing panel. Attachment points for these cables were located on the wing at chordwise locations approximately $0.23\bar{c}$ and $0.60\bar{c}$ at a spanwise point approximately 4 feet from the fuselage beneath the point where buckling was first observed. The front cable was rigged taut to take load and the rear cable was left slack to serve only to reduce wing motion should buckling occur. This approach was taken as it was felt that adding the cable near the center of pressure should provide the necessary restraint and offer the greatest chance of reducing unfavorable wing twist on the inboard wing sections.

The results of the tests made at normal inflation pressure (7 lb/sq in.) with the additional guy cables installed (fig. 6) showed an appreciable improvement in the aerodynamic characteristics along with higher load capability. For this configuration the degree of instability resulting at the higher loadings is greatly reduced and the increase in lift-curve slope with speed was noticeably less. Also for the higher speed condition, wing buckling finally occurred only after a condition of intermittent stall of the left wing developed which produced a series of wing oscillations which were followed by buckling along a chordwise line approximately 2 feet out from the fuselage center line. For this configuration a lift load of approximately 1,300 pounds was recorded for an airplane attitude approximately 1° below stall ($\alpha = -3.1^\circ$). Stall and buckling occurred as the airplane attitude was further increased to -2.1°. Loads for this condition can only be estimated but it is reasonable to believe that a value of $C_{L,max}$ of at least 1.0 was reached with the maximum load approaching 1,400 pounds for a load factor of approximately 2.5.

Although buckling occurred at this condition, it is conceivable that the longer time lapse and the intermittent stall preceding buckling would be an effective warning of the approaching buckling boundary. It is also felt that by further modification to the wing-guy-cable and wing-root attachments, additional improvements in the stability and load limit could probably be obtained; however, such development was beyond the intended scope of this program.

As an additional point of interest in connection with load characteristics of the pneumatic structure, a short series of tests was made with wing and fuselage pressures reduced from normal pressure to ascertain the possibility of maintaining flight near minimum speed in case of an emergency caused by loss of air pressure. The results of the reduced pressure tests (fig. 7) did not show any drastic changes in aerodynamic characteristics which should rule out flight down to the lowest test pressure of 3 lb/sq in. At this pressure the wing did not buckle for the test speed with the maximum load factor reaching approximately 1, and brief aileron and elevator control checks indicated that control could be maintained.

Wing-Guy-Cable Loads and Deflection Studies

Loads measured in the wing guy cables for the two cable configurations tested are summarized in figures 8 and 9 where the individual cable loads are plotted as a function of total configuration lift. Wing-deflection photographs for some of the more pertinent conditions are presented in figures 10 to 14. These photographs have airplane angle of attack and total configuration lift noted on each to permit correlation with the proper cable loads and aerodynamic data plots. Horizontal stripes on the vertical deflection target bar shown at the wing tips in the photographs are spaced 2 inches apart. The long stripe on the horizontal bar provided general horizontal reference.

The cable-load data for the original configuration (fig. 8) indicate that the wing bending due to lift is primarily restrained by the front guy cables and the bending due to chordwise forces by the rear guy cables. At zero lift the rear-guy-cable load is therefore larger than the front-cable load at all speeds; but as lift is increased, the front-cable load increases rapidly and for the high loading condition (fig. 8(d)) the front-cable loads reach values over three times as large as the rear-cable loads. With this cable configuration the front-cable load was approximately twice the rear-cable load for the 1 g condition (550-pound lift) condition at all test speeds.

Cable-load data for the modified cable system (fig. 9) show that the additional cable attached forward and inboard on the wing

appreciably reduced the load in the original front guy cable at the higher load conditions but had only a small effect on the rear-cable load. The maximum load reached on the inboard cable was approximately 200 pounds for the maximum loading condition (fig. 9(c)) which imposed loads of over 600 pounds on the outboard front wing cable. The inboard cable could probably have been made to carry more load by preloading; however, the additional cable as installed raised the allowable wing load to a value slightly above stall onset at maximum design speed (71 mph). If a higher allowable load is required, it is felt that some further improvement could best be obtained by adding another light guy cable at the new initial failure point which for the modified cable system was approximately 2 feet out from fuselage center line.

The wing-deflection photographs for the two cable systems at all speeds tested (figs. 10 to 14) show only small differences in deflection for the two cable systems at load conditions approximating steady level flight (L = 550 pounds). At the higher loading conditions obtained at the higher speeds, however, the wing deflections are noticeably different. For the original cable installation the deflection inboard is seen to build up with load (fig. 12) until failure is reached at a load just over 1,100 pounds. For the modified cable system at the same speed (fig. 14) the deflection inboard is less and at the higher loadings reached with this cable system the tip sections show a more pronounced deflection.

Control Characteristics

The static longitudinal characteristics of the airplane with the elevators deflected are presented in figure 15 for test speeds averaging 41 and 64 miles per hour. The data for these speeds chosen to represent minimum-speed and cruising-speed flight conditions, respectfully, show a marked change in static stability with speed but little change in the effectiveness of the elevator to produce trim. Comparison of the elevator angles obtained for a given deflection of the control stick indicated somewhat lower response of control motion to a given stick motion at the higher speeds. Adequate control would appear to be available, however, and the loss of response is apparently the result of stretch within the semirigid control system at higher loads. The amount of twist occurring in the elevator control surface was small as may be seen in figure 15.

Longitudinal and lateral aerodynamic data obtained with the ailerons deflected for the same test velocities previously discussed are shown in figures 16 and 17. A reduction in rolling-moment coefficient for a given stick deflection is evident at the higher speed condition. This reduction apparently comes from aeroelastic effects and from a reduction in control motion with stick deflection at the higher loading condition.

The reduced control motion is most apparent for the up-aileron in all cases because the up-aileron is acutated by a simple bungee cord attached to the upper surface so that preset tension in this cord pulls the control up when tension is relaxed in the lower actuating cable by deflection of the stick. Rolling-moment coefficients higher than those shown for the condition at $q_{av} = 10$ could have been obtained by utilizing full control travel; however, with the model rigidly mounted through the fuselage for these tests, a nondesign condition existed with the wing rolling moment applied with fuselage restrained. Maximum rolling-moment tests, therefore, were not made at the higher speed.

SUMMARY OF RESULTS

The results of tests on the Goodyear Inflatoplane may be summarized as follows:

1. The airplane, with original guy cables, was stable through stall for low speed conditions but for the higher speed conditions exhibited instability in the lift-coefficient range representing load factors greater than 1.

2. With the original wing-guy-cable configuration, wing stall occurred without any wing buckling for test speeds to 64 mph (load factor just under 2) but at approximately 70 mph wing buckling occurred with a load factor slightly higher than 2.

3. The longitudinal instability noted for the higher load factor conditions was apparently the result of increased wing incidence inboard due to growth and stretch in the nylon fabric.

4. Wing buckling which occurred as a column type failure inboard approximately midway between the fuselage and wing-guy-cable attachment points resulted in the inboard wing sections folding upward in a manner to bring them within the propeller disk area. When wing puncture did not occur due to contact with the engine (without propeller), wing recovery from a buckled condition was instantaneous with load reduction and without apparent damage.

5. The addition of one wing guy cable attached on the lower wing surface at the point of initial buckling appreciably reduced the static longitudinal instability at higher speeds and allowed the airplane to reach stall at 70 mph before buckling occurred. Buckling followed the wing oscillations produced by stall. Maximum lift loads reached approximately 1,400 pounds (load factor approximately 2.5) before stall.

6. For all configurations studied, the wing behavior following buckling was such that an operating propeller would have struck and destroyed the wing.

7. Tests made with airplane inflation pressure reduced and air speeds considered minimum for maintaining level flight indicate that flight should be possible in an emergency for inflation pressures less than one-half the normal inflation pressure.

8. Elevator and aileron control characteristics were modified somewhat by changes in speed due to flexibility in the structure and control system; however, adequate control should be maintained throughout the design speed range.

Langley Aeronautical Laboratory,
National Advisory Committee for Aeronautics,
Langley Field, Va., April 17, 1958.

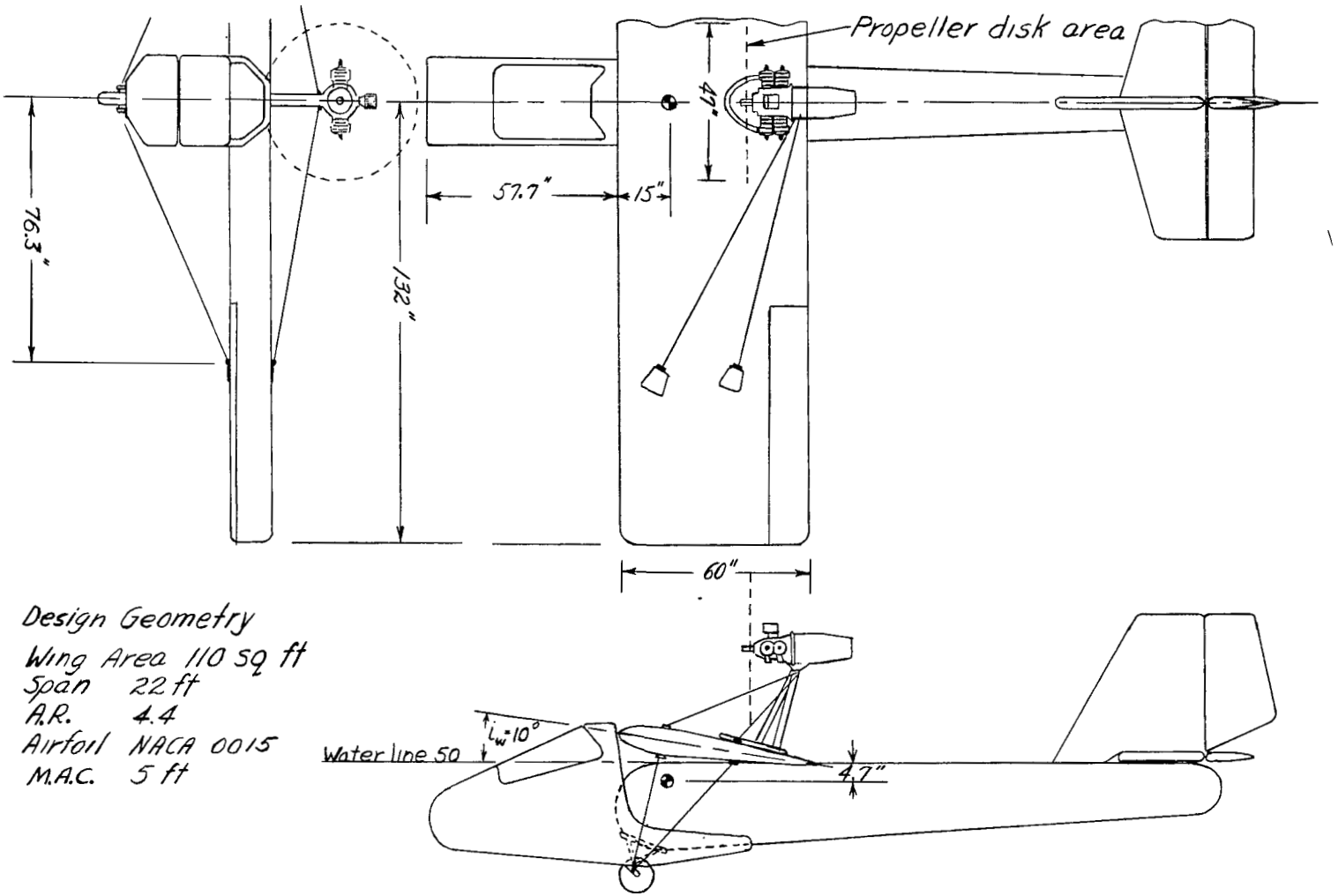

Figure 1.- Geometric characteristics of the Goodyear Inflatoplane.

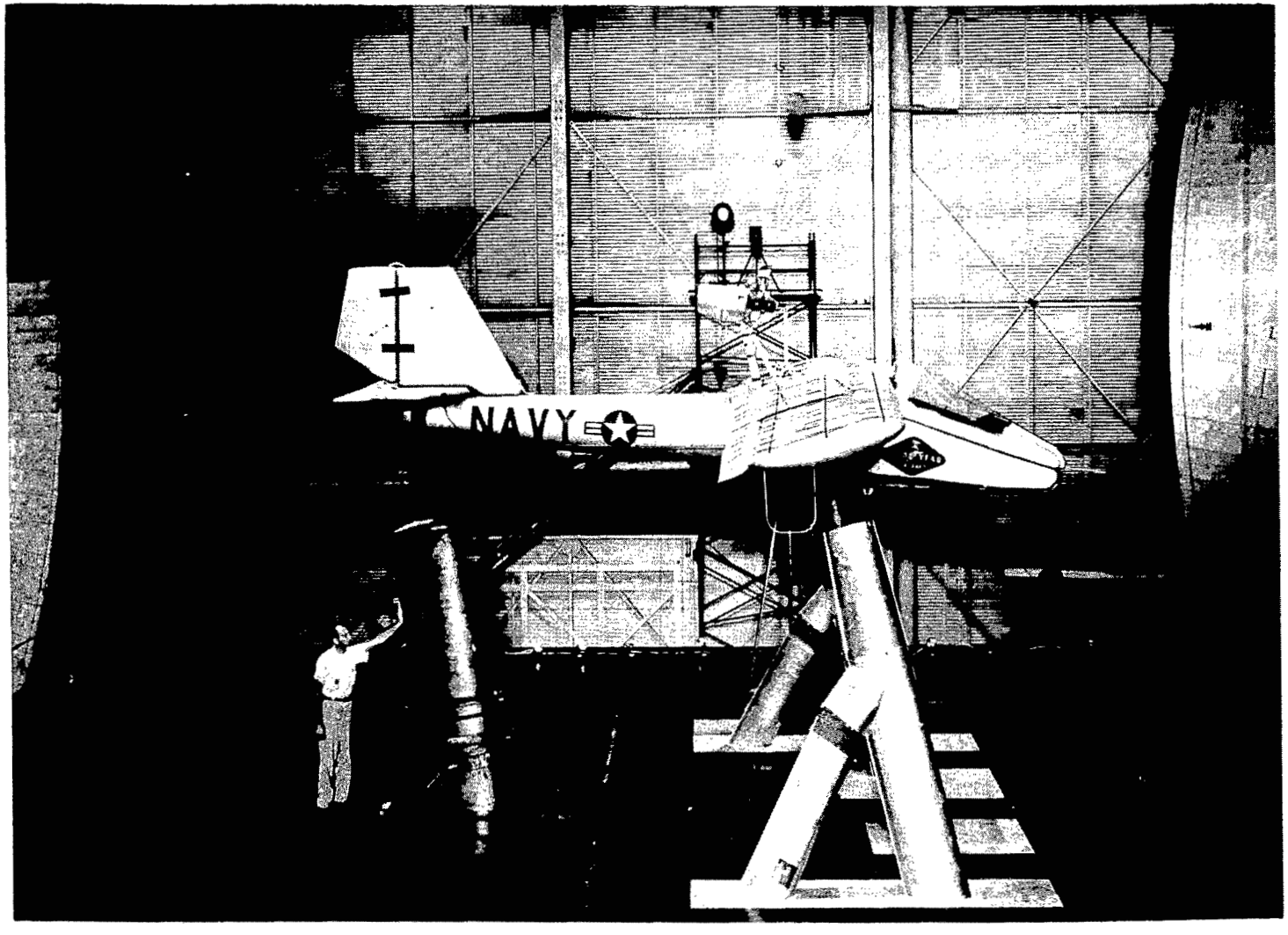

Figure 2.- Goodyear Inflatoplane in the Langley full-scale tunnel. L-57-3490

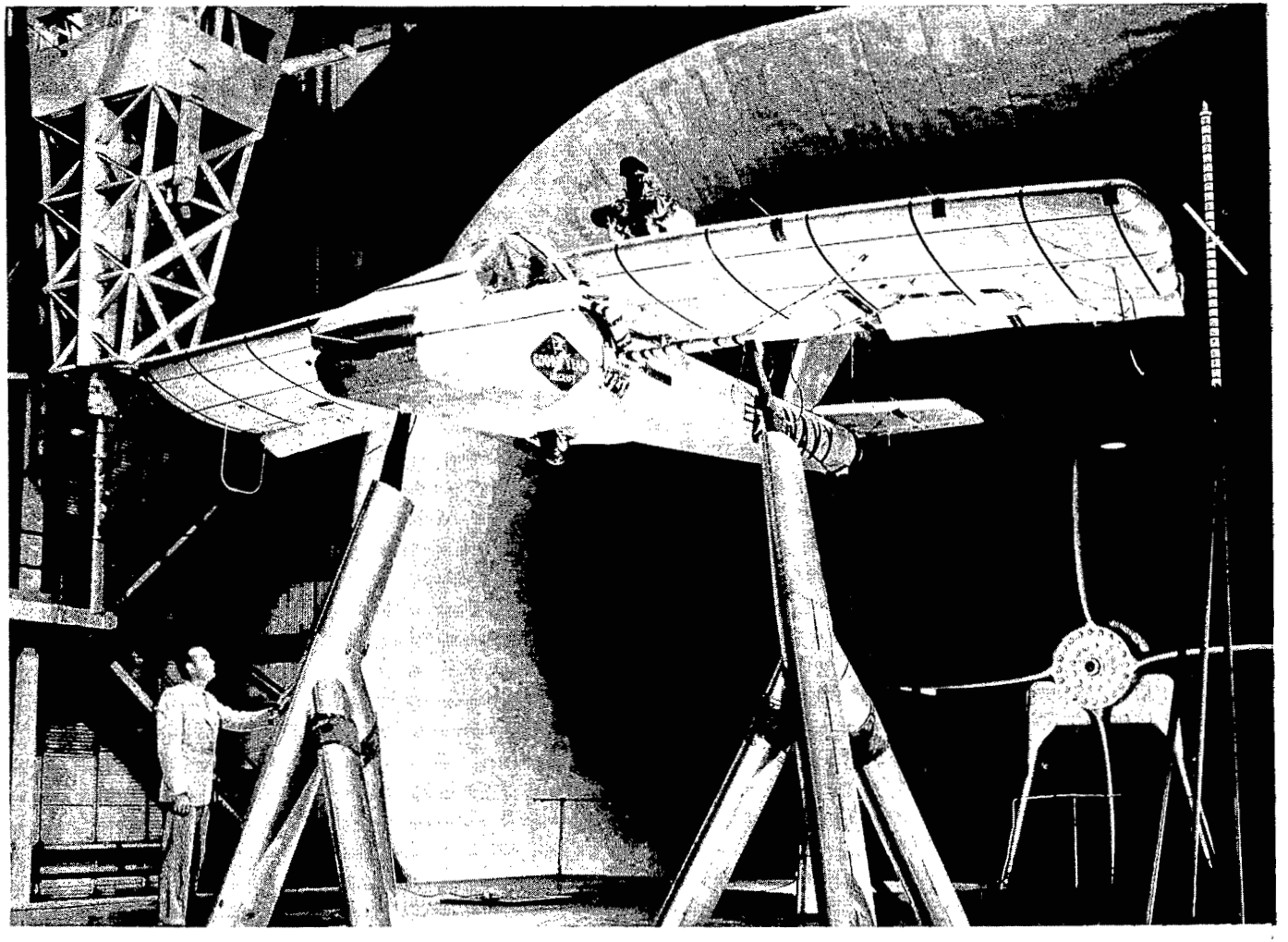

(a) General view. L-57-3414

Figure 3.- Inflatoplane mounting arrangement.

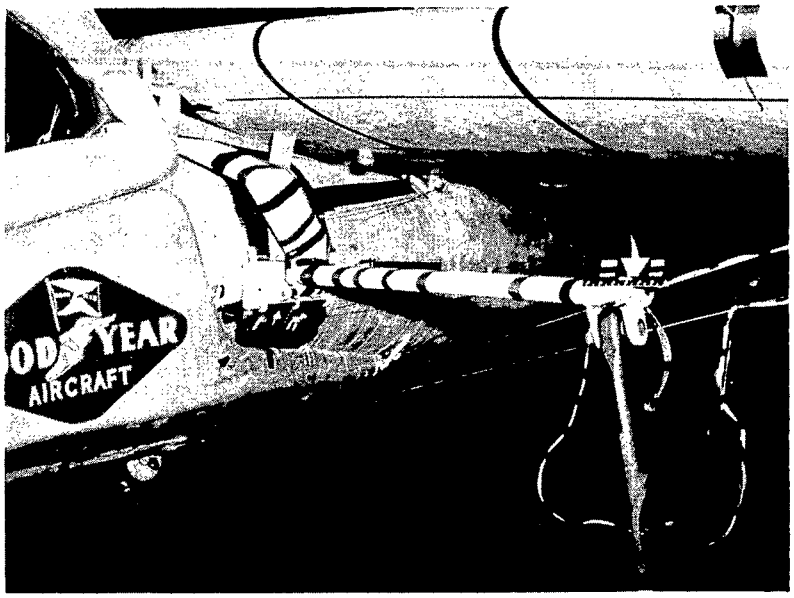

(b) Main support yoke. L-57-3495

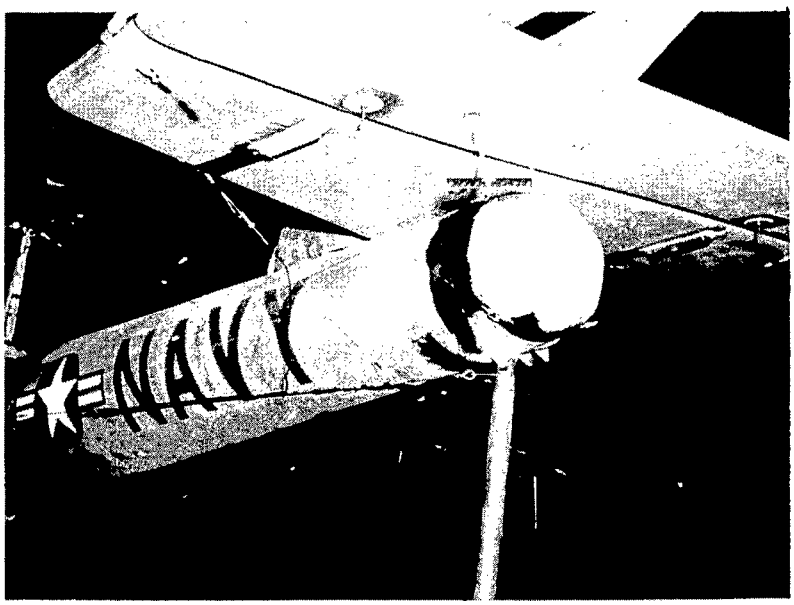

(c) Tail support fitting. L-57-3496

Figure 3.- Concluded.

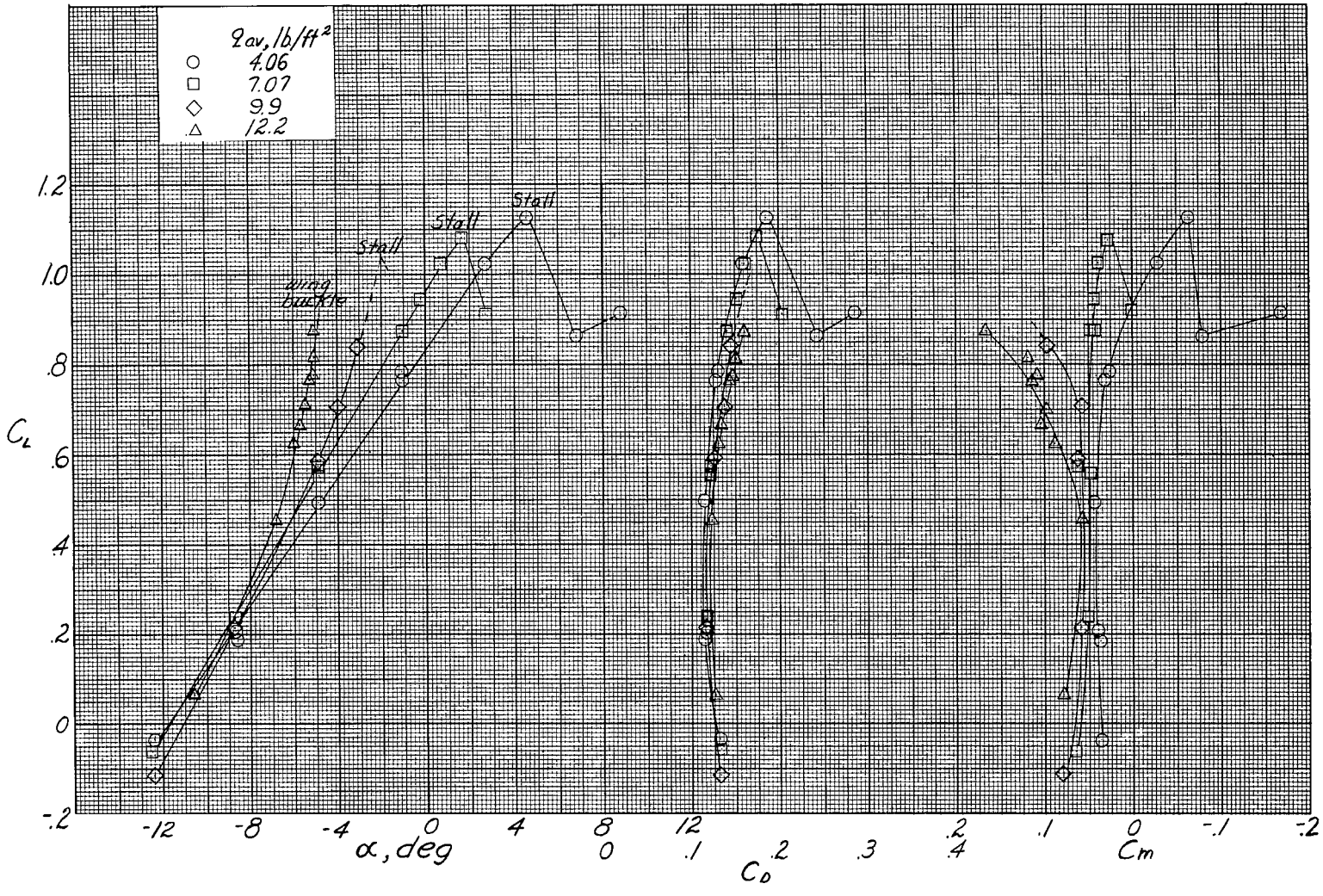

Figure 4.- Aerodynamic characteristics of the Goodyear Inflatoplane at several wind velocities. Original configuration; normal inflation pressure (7 lb/sq in.); controls neutral; canopy installed.

(a) At failure. L-57-3524

Figure 5.- Wing buckling sequence.

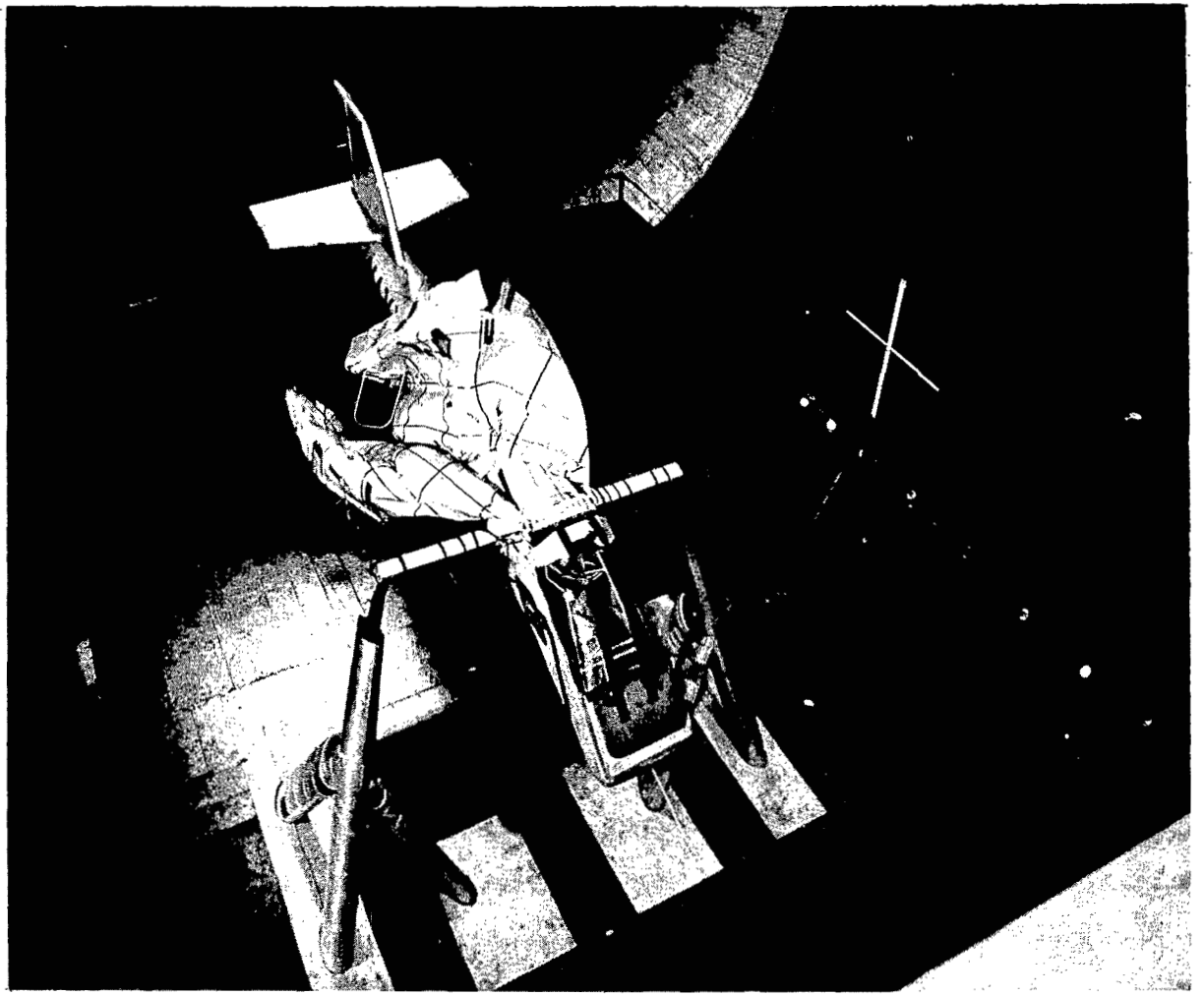

(b) After puncture. L-57-3525

Figure 5.- Concluded.

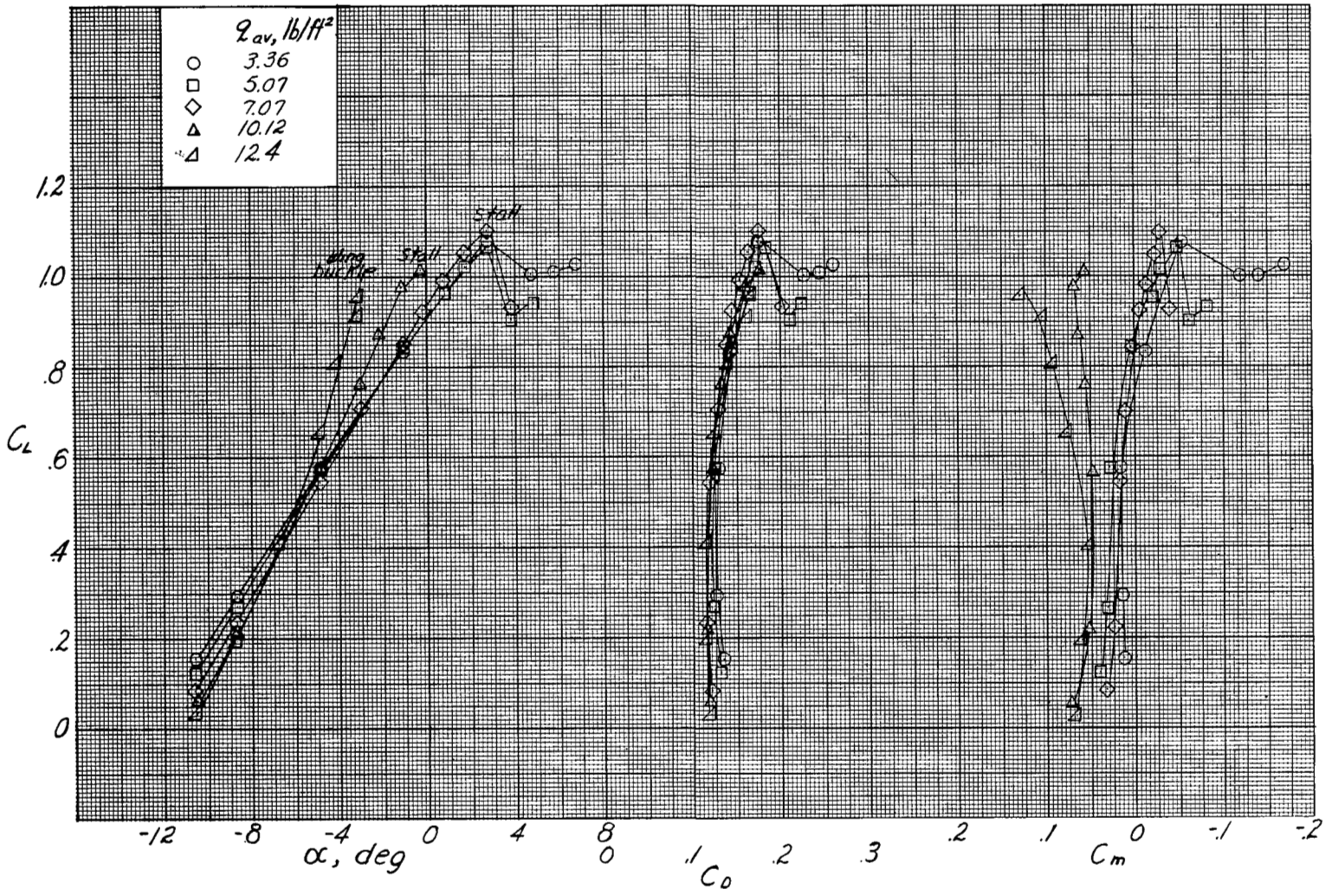

Figure 6.- Aerodynamic characteristics of the Goodyear Inflatoplane at several tunnel velocities. Additional wing guy cables installed; normal inflation pressure (7 lb/sq in.); controls neutral; canopy installed.

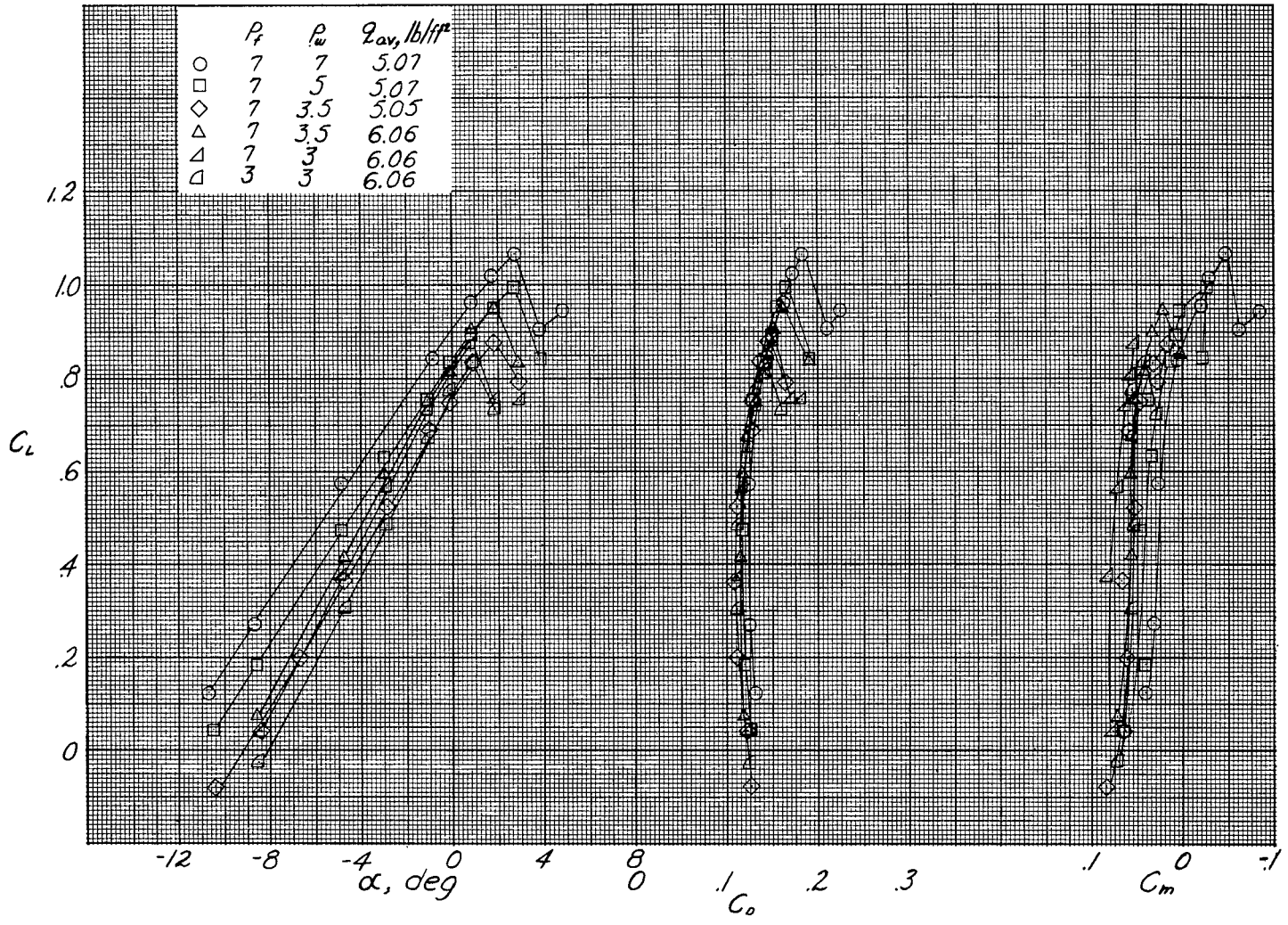

Figure 7.- Aerodynamic characteristics of the Goodyear Inflatoplane with variations in the wing and fuselage inflation pressure. Additional wing guy cables installed; controls neutral; canopy installed.

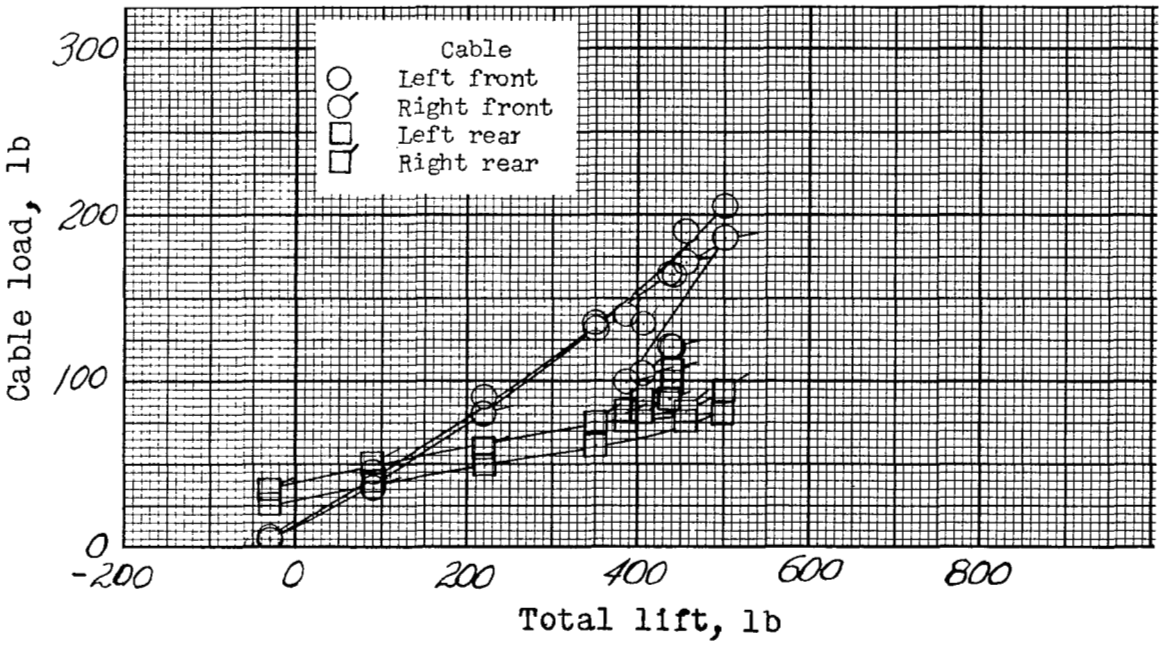

(a) V = 41 mph; q_{av} = 4.06 lb/sq ft.

Figure 8.- Variation of wing-guy-cable loads with airplane total lift for several wind velocities. Original configuration; normal inflation pressure (7 lb/sq in.); controls neutral.

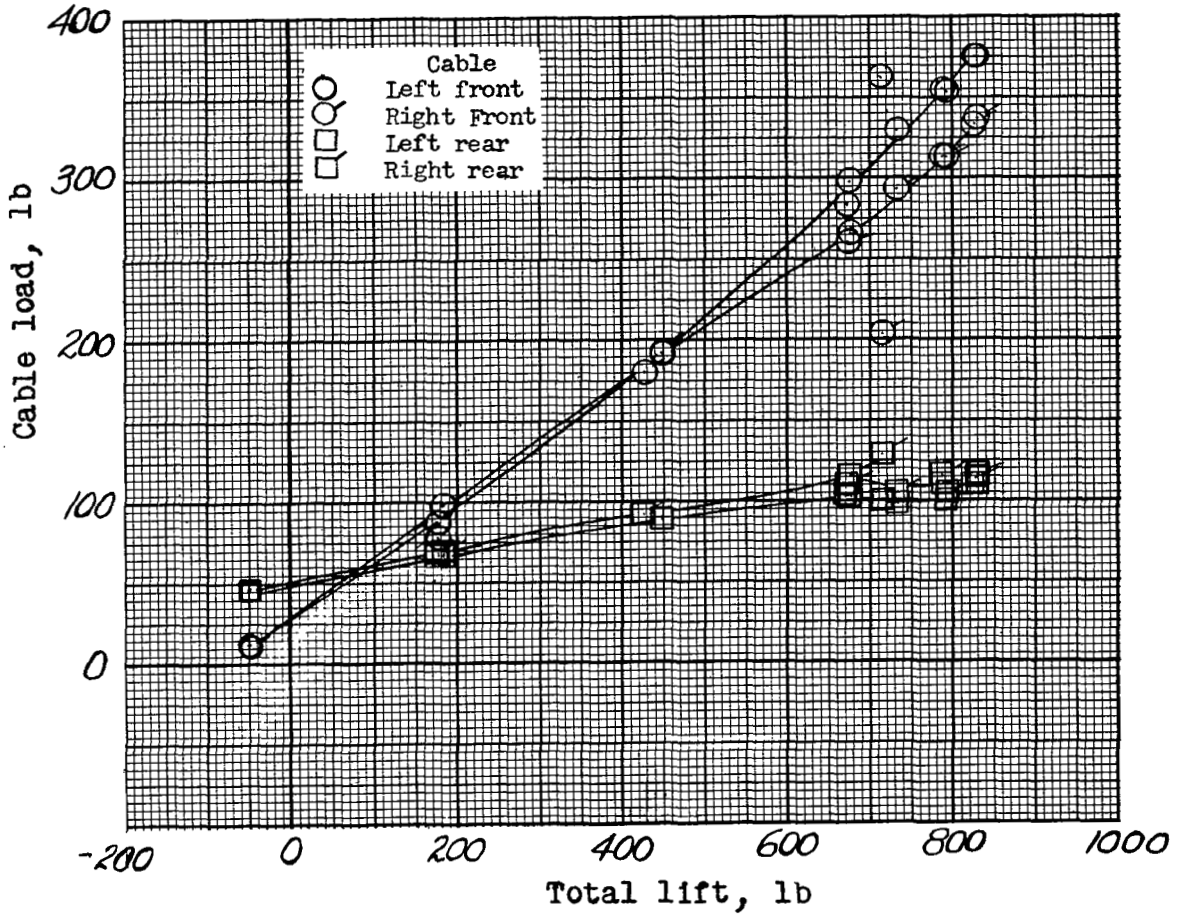

(b) V = 54 mph; q_{av} = 7.07 lb/sq ft.

Figure 8.- Continued.

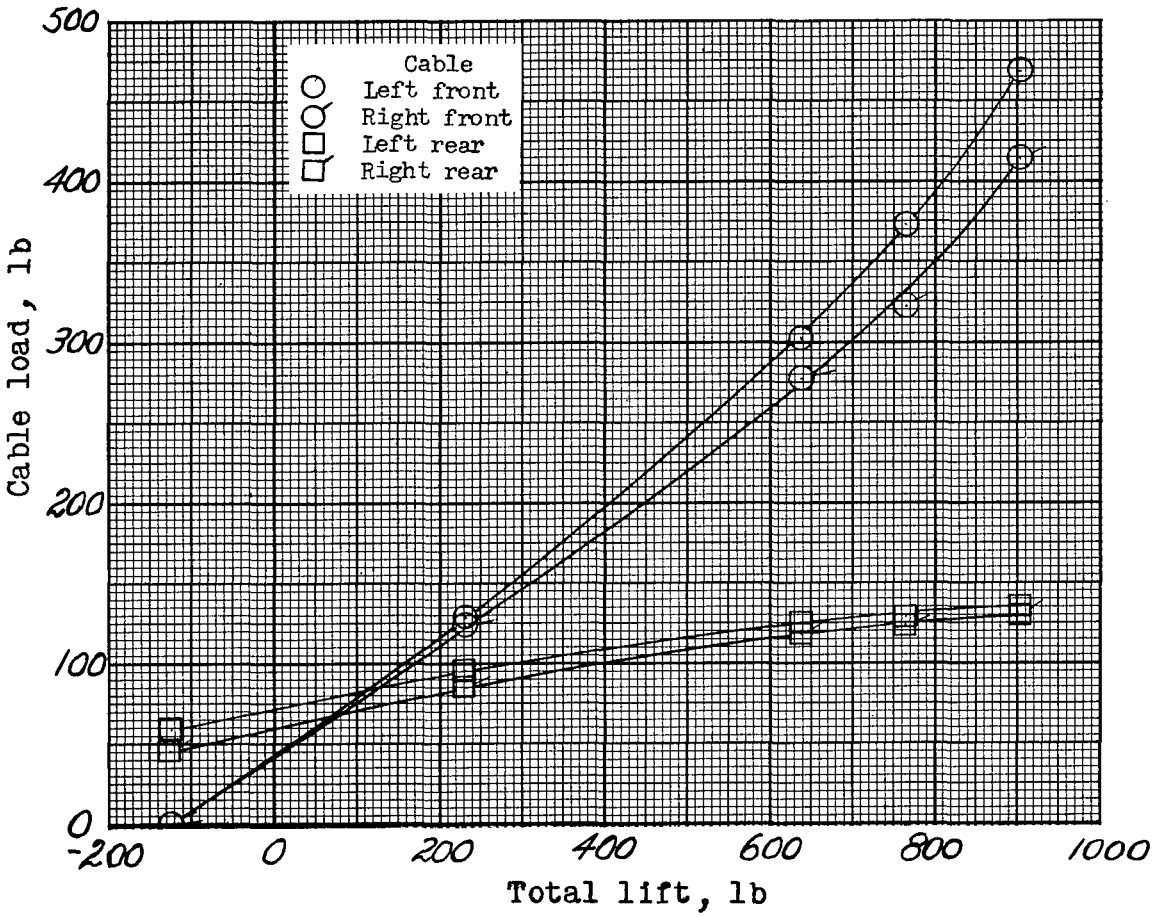

(c) V = 64 mph; q_{av} = 10.15 lb/sq ft.

Figure 8.- Continued.

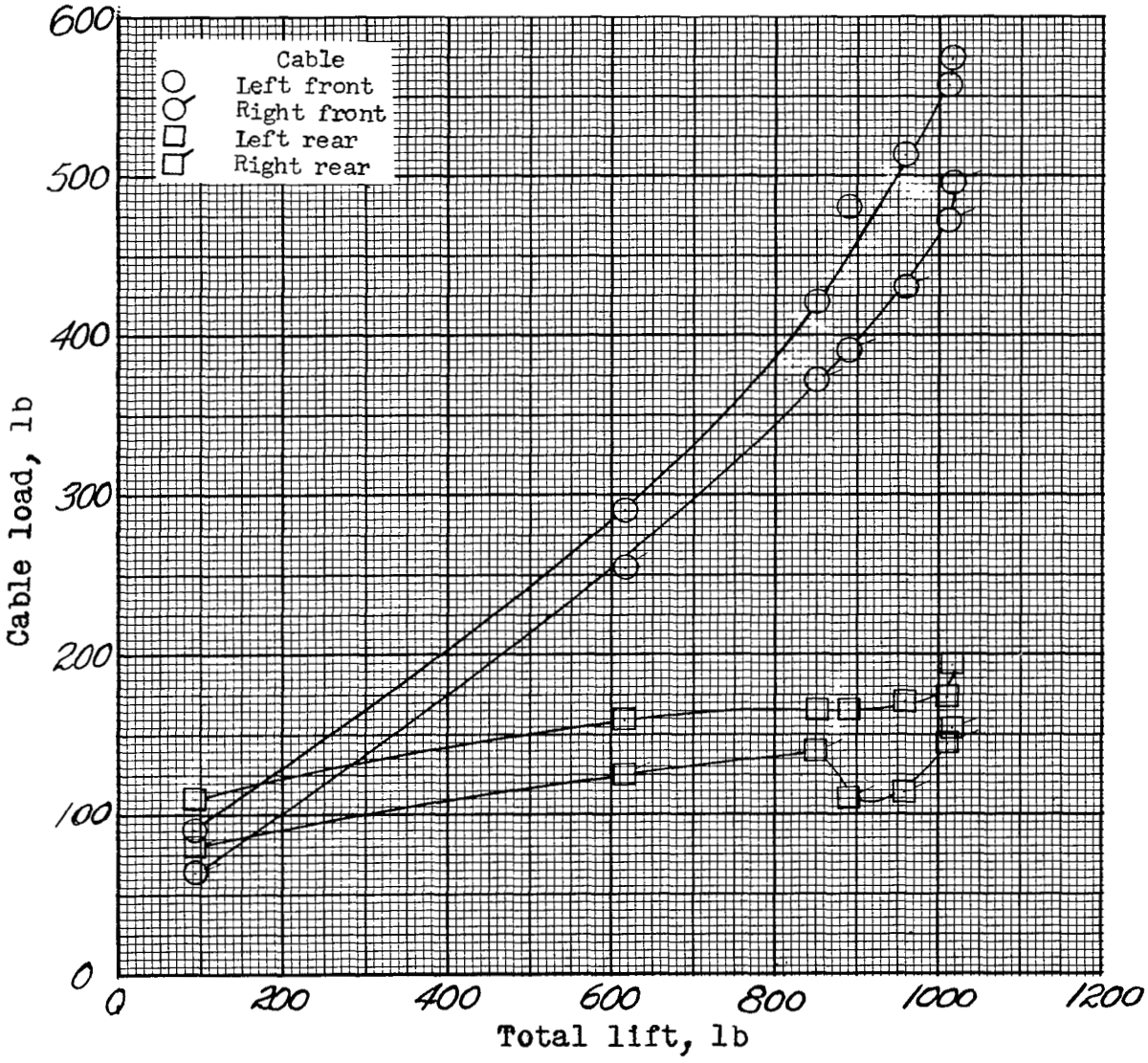

(d) V = 71 mph; q_{av} = 12.2 lb/sq ft.

Figure 8.- Concluded.

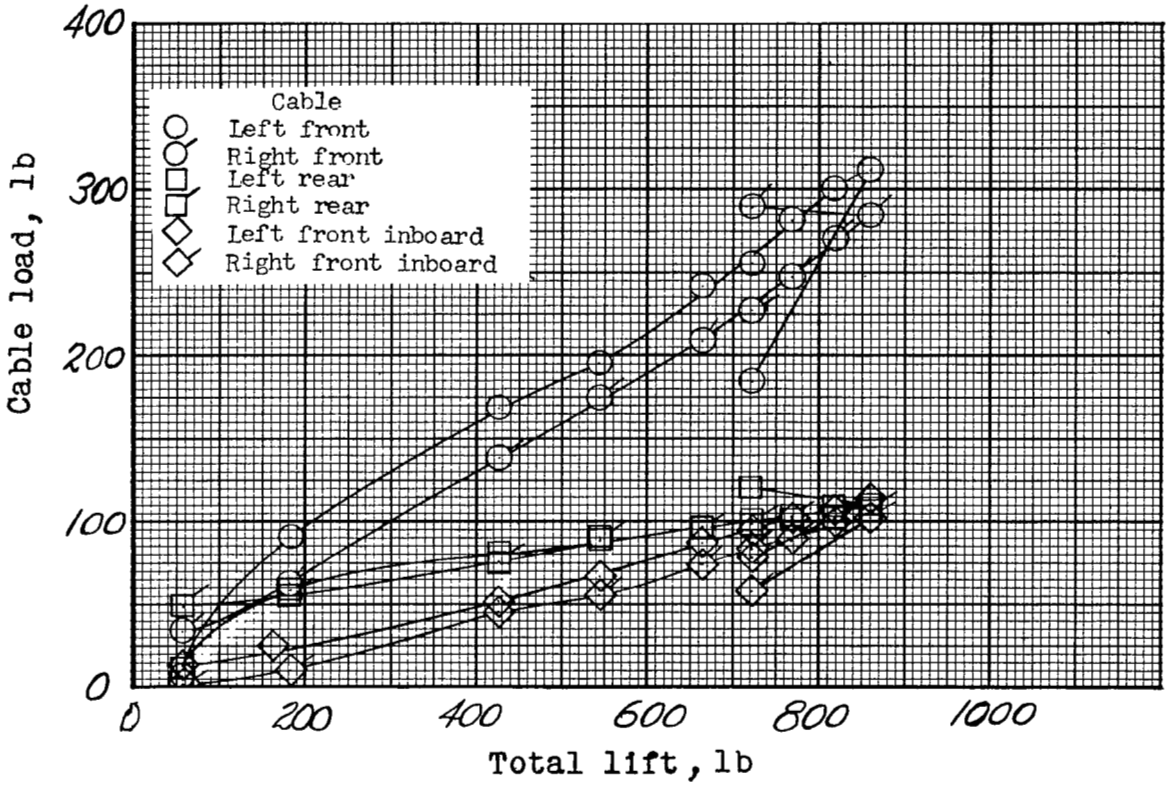

(a) V = 54 mph; q_{av} = 7.07 lb/sq ft.

Figure 9.- Variation of wing-guy-cable loads with airplane total lift for several wind velocities. Additional wing guy cables installed; normal inflation pressure (7 lb/sq in.); controls neutral.

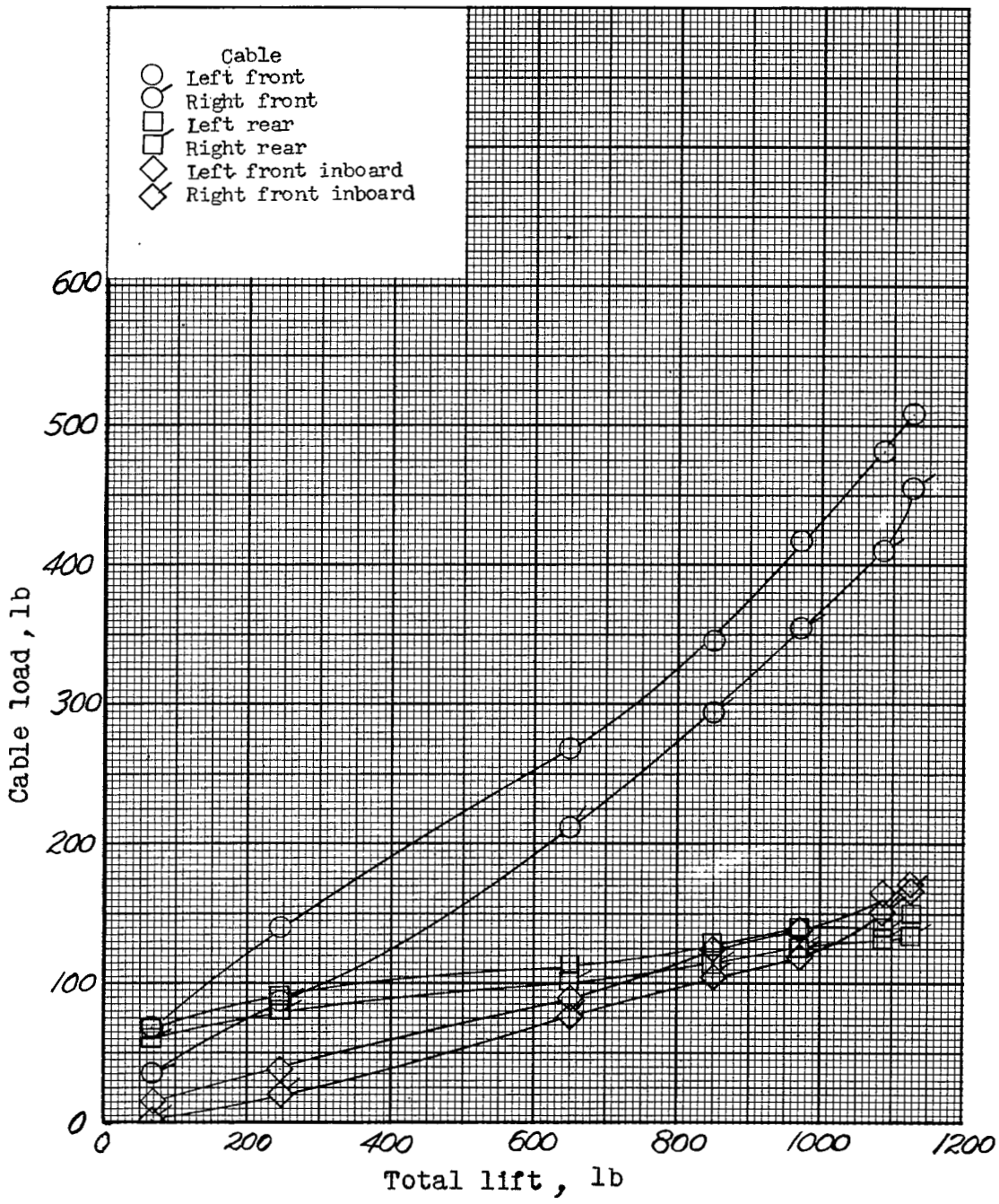

(b) V = 64 mph; q_{av} = 10.15 lb/sq ft.

Figure 9.- Continued.

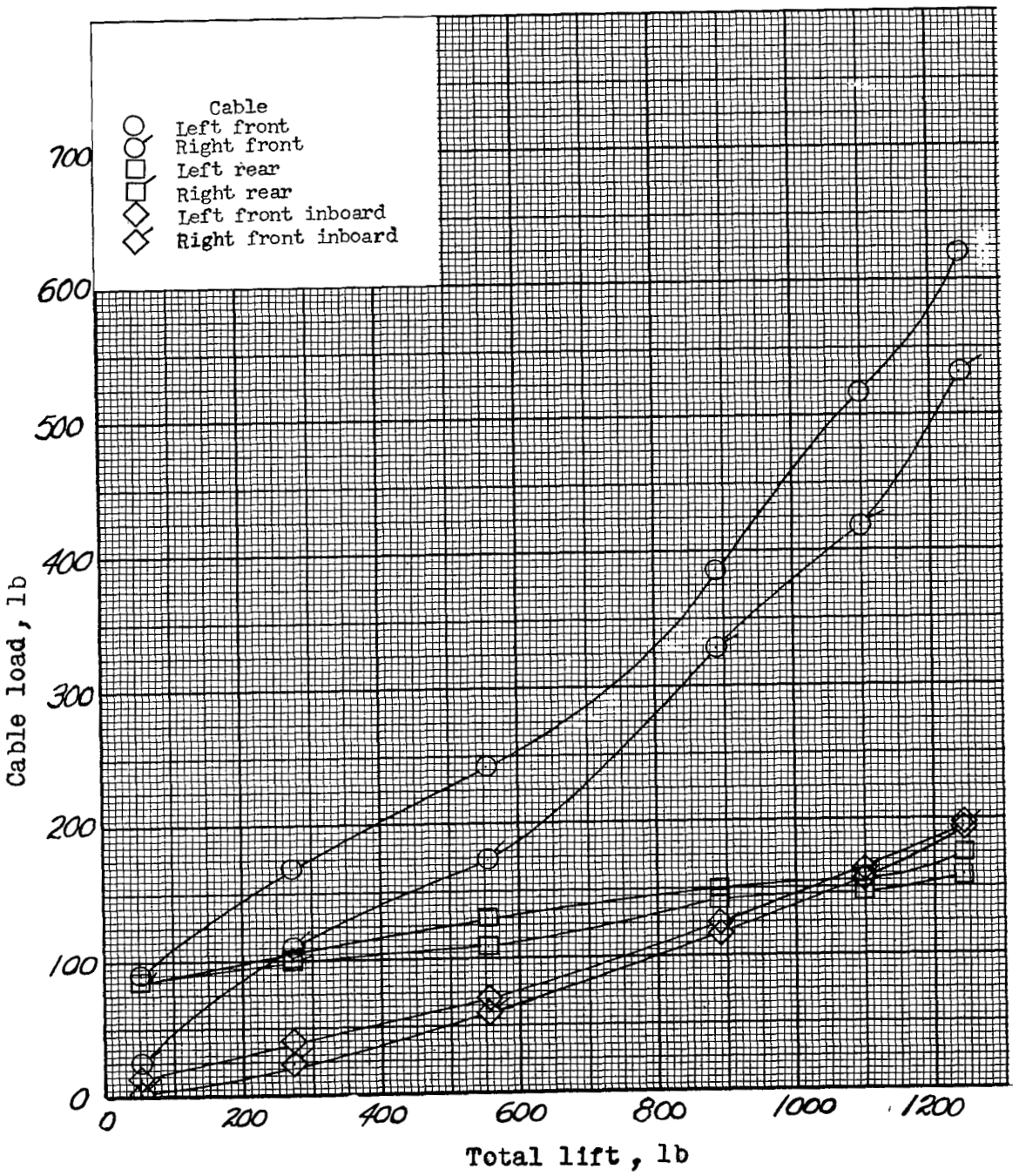

(c) V = 71 mph; q_{av} = 12.4 lb/sq ft.

Figure 9.- Concluded.

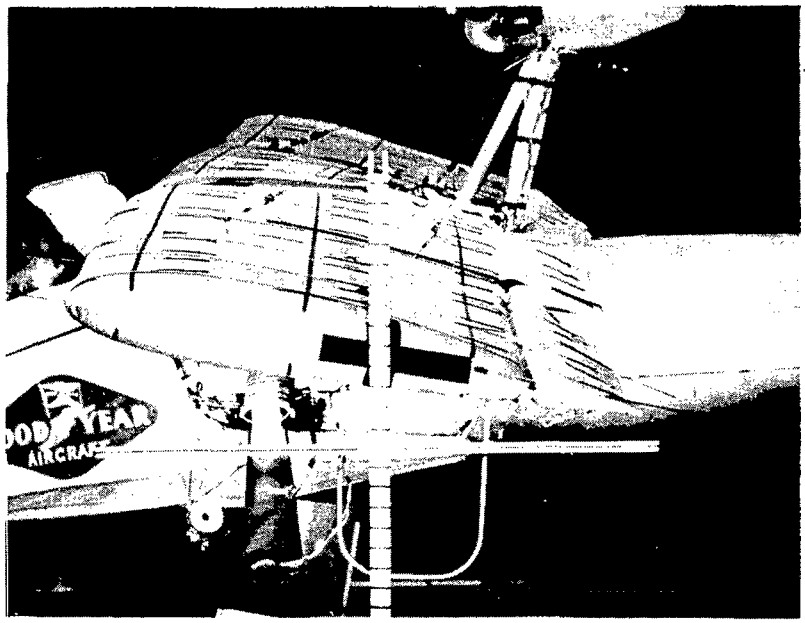

Upper camera; $\alpha = -3^{\circ}$; L = 562 lb.

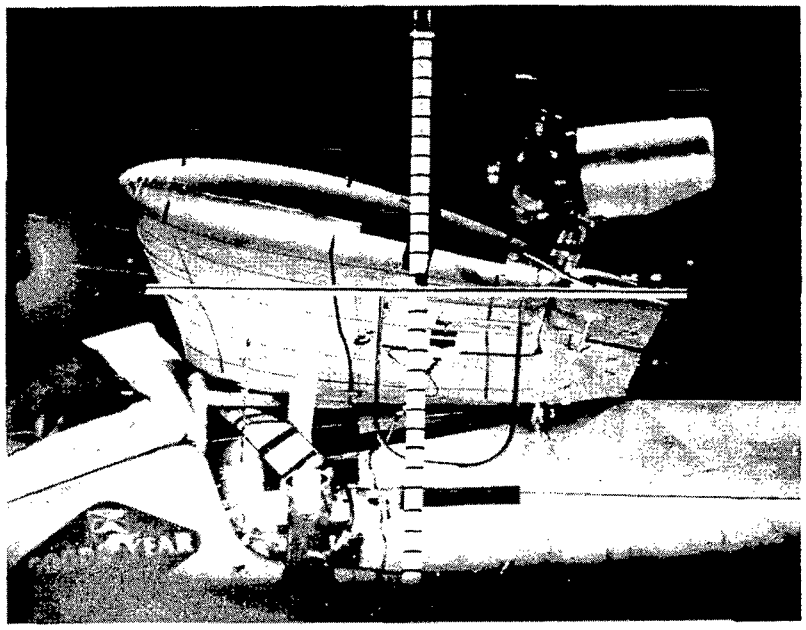

Lower camera; $\alpha = -3^{\circ}$; L = 562 lb. L-58-1633

Figure 10.- Deflection study photographs for original configuration. V = 54 mph; q_{av} = 7.07 lb/sq ft.

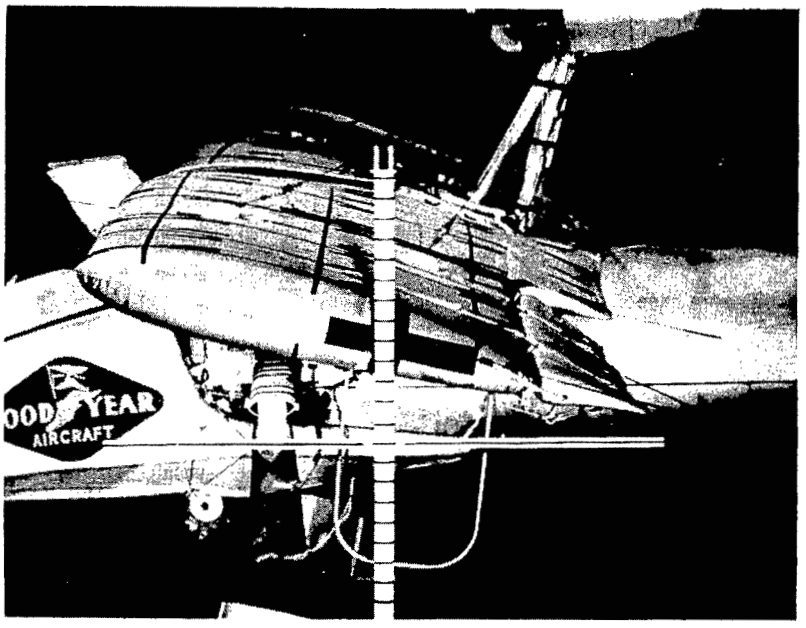

Upper camera; $\alpha = -1.2^{\circ}$; L = 676 lb.

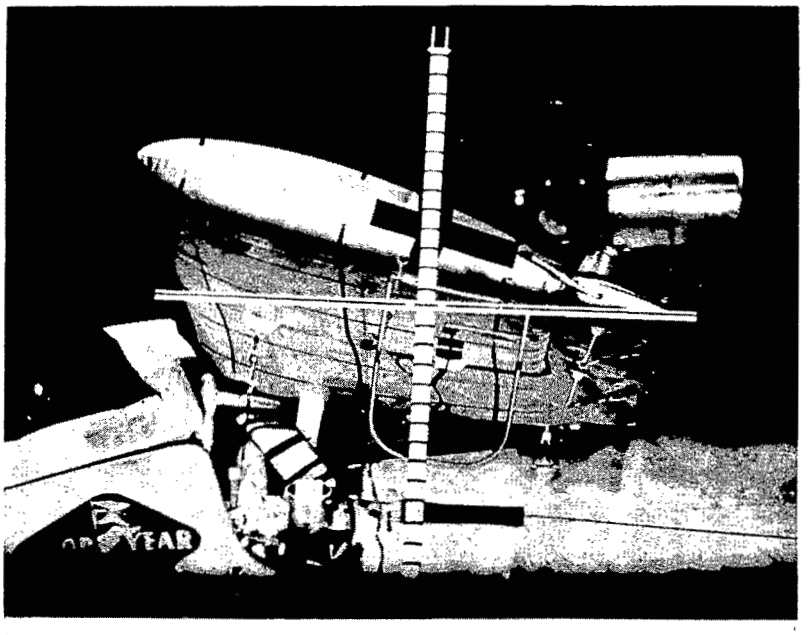

Lower camera; $\alpha = -1.2^{\circ}$; L = 676 lb. L-58-1634

Figure 10.- Continued.

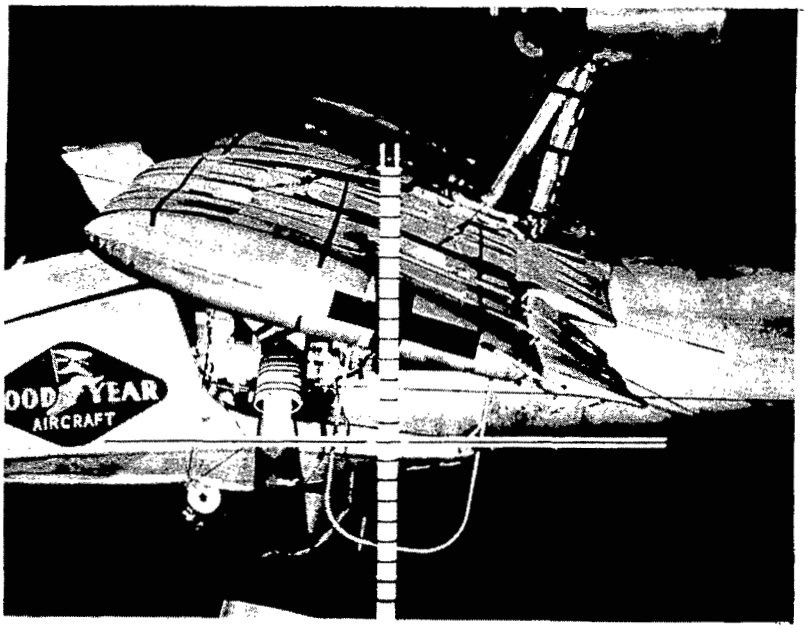

Upper camera; $\alpha = 0.7^{\circ}$; L = 7.88 lb.

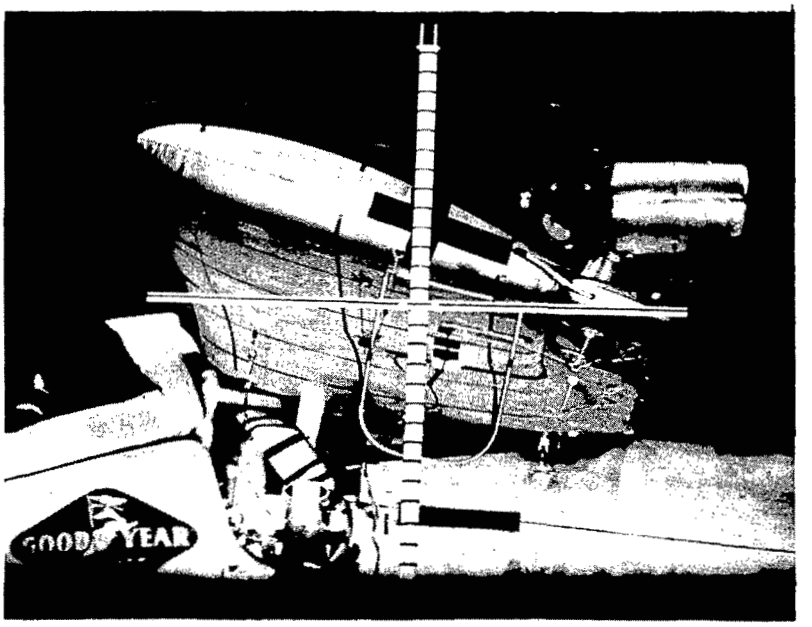

Lower camera; $\alpha = 0.7^{\circ}$; L = 788 lb. L-58-1635

Figure 10.- Continued.

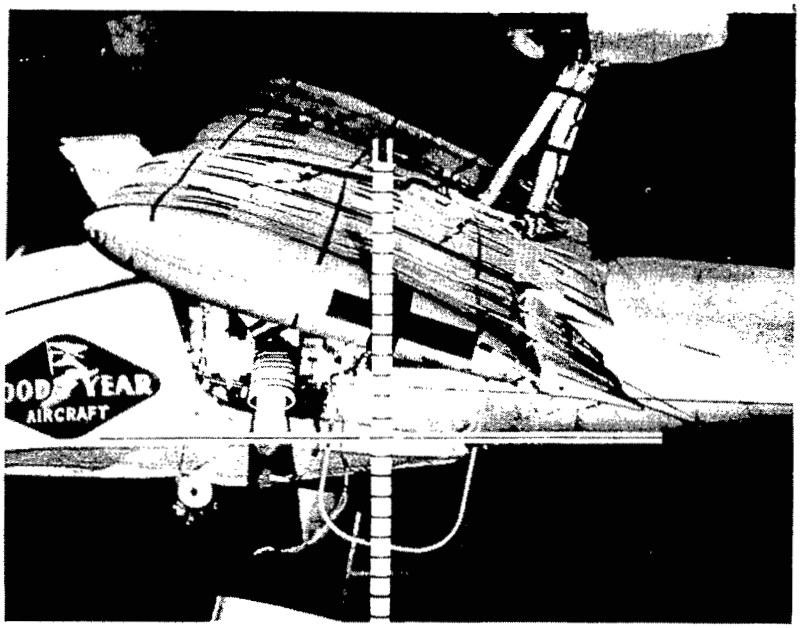

Upper camera; $\alpha = 1.7^{\circ}$; L = 830 lb.

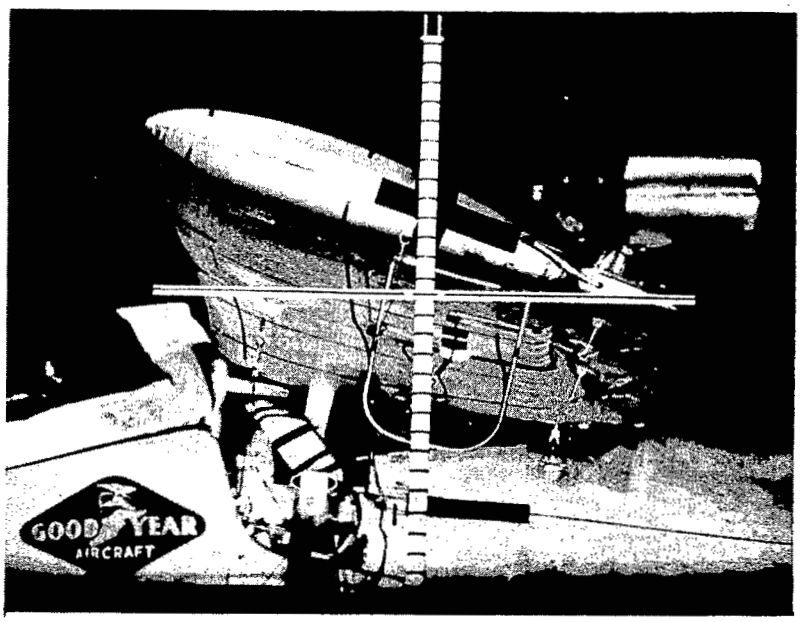

Lower camera; $\alpha = 1.7^{\circ}$; L = 830 lb. L-58-1636

Figure 10.- Concluded.

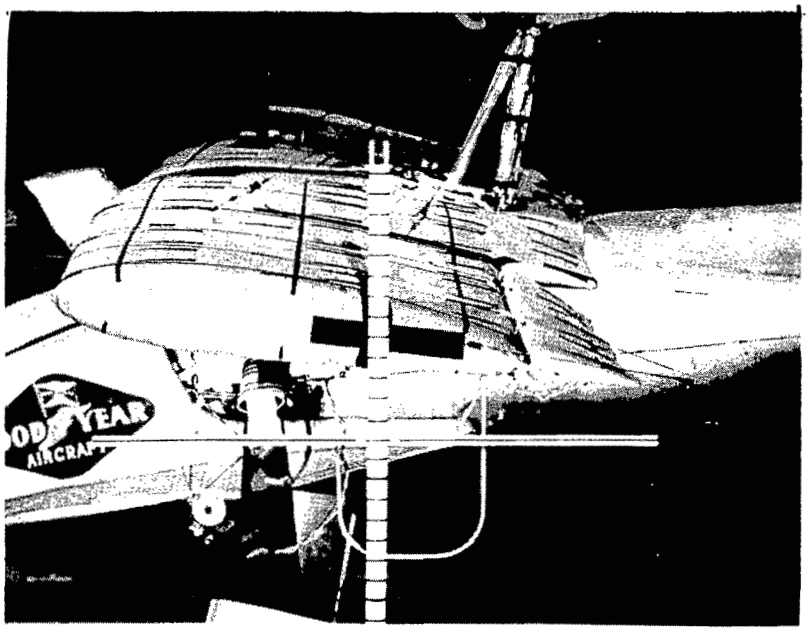

Upper camera; $\alpha = -5.8^{\circ}$; L = 537 lb.

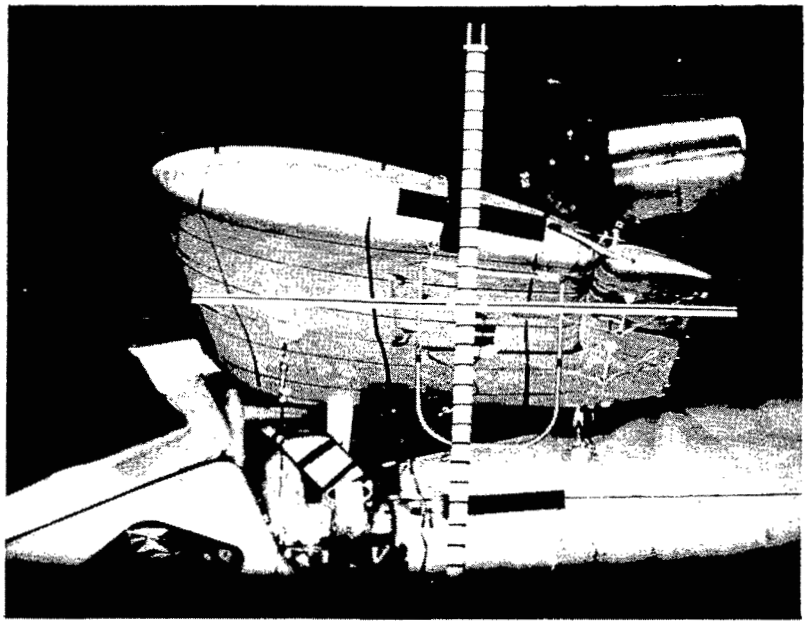

Lower camera; $\alpha = -5.8^{\circ}$; L = 537 lb. L-58-1637

Figure 11.- Deflection study photographs for original configuration. V = 64 mph; q_{av} = 10.15 lb/sq ft.

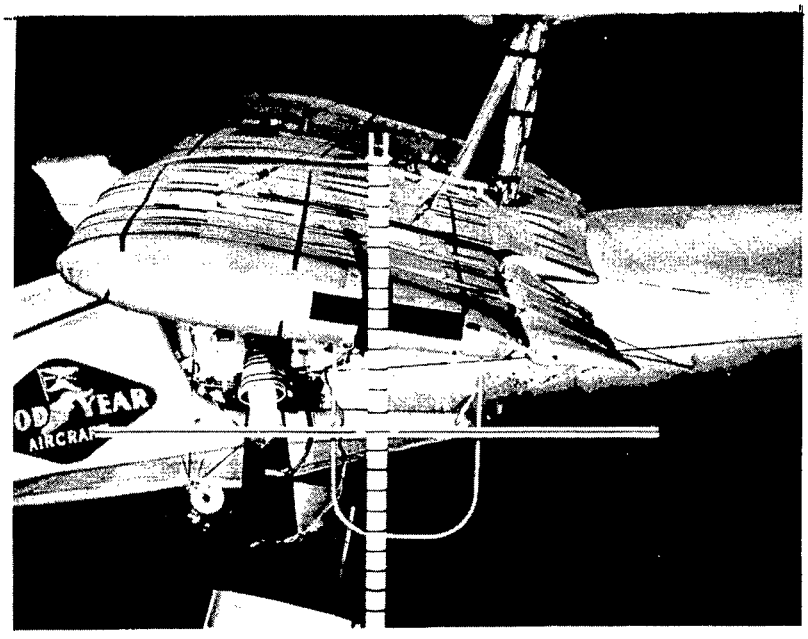

Upper camera; $\alpha = -4.9^{\circ}$; L = 639 lb.

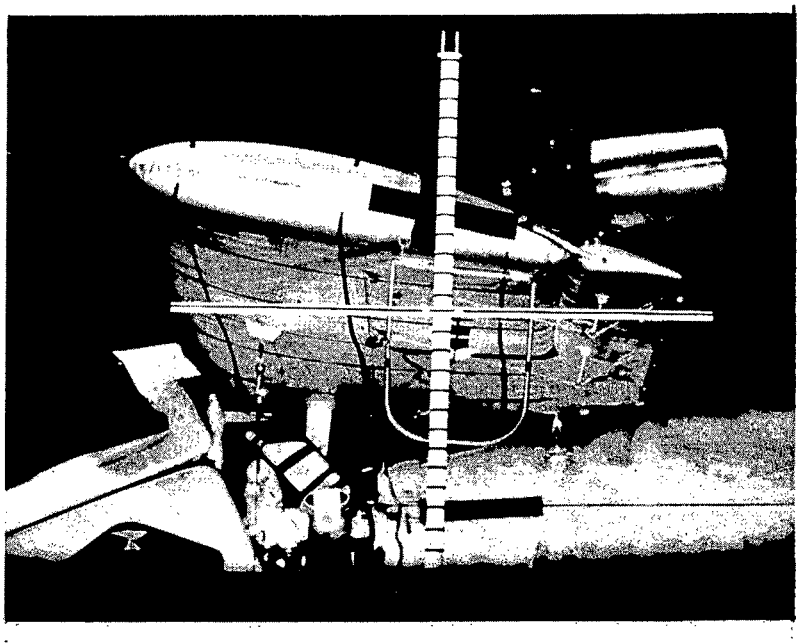

Lower camera; $\alpha = -4.9^{\circ}$; L = 639 lb. L-58-1638

Figure 11.- Continued.

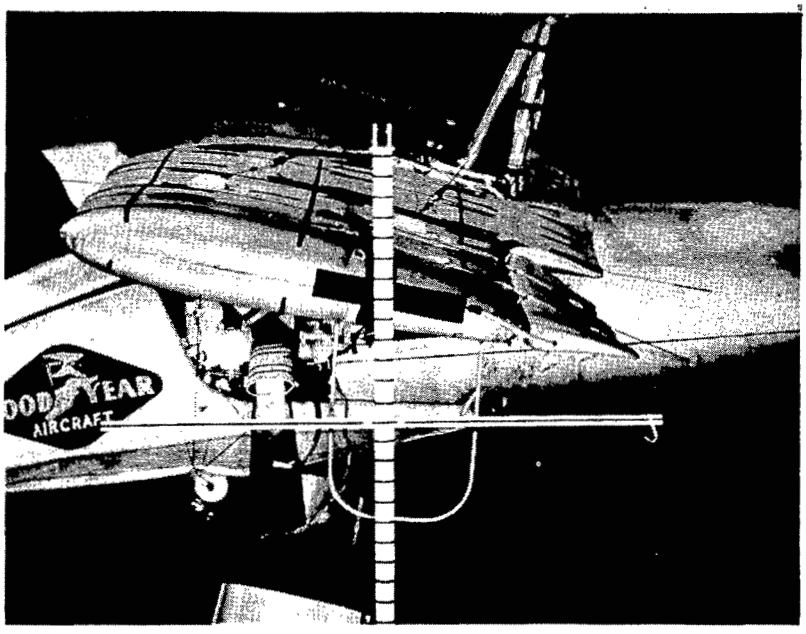

Upper camera; $\alpha = -4^{\circ}$; L = 765 lb.

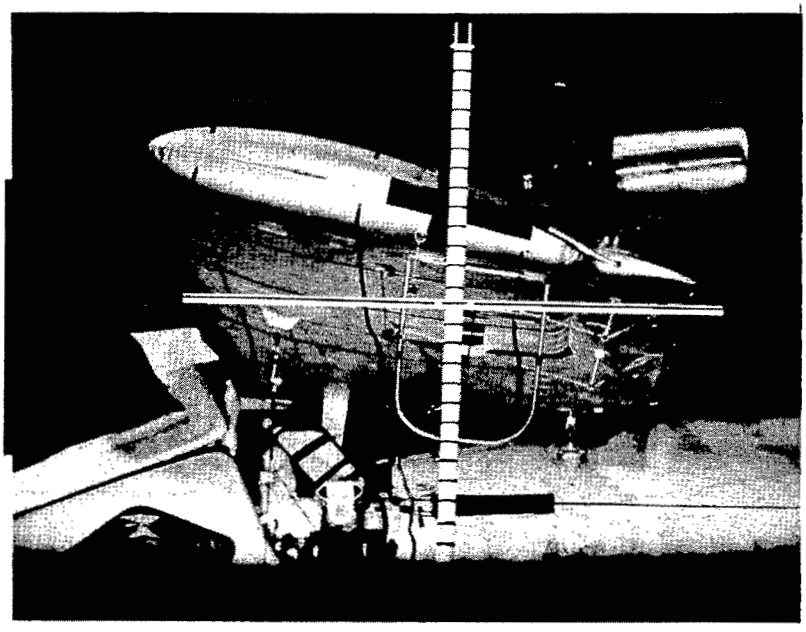

Lower camera; $\alpha = -4^{\circ}$; L = 765 lb. L-58-1639

Figure 11.- Continued.

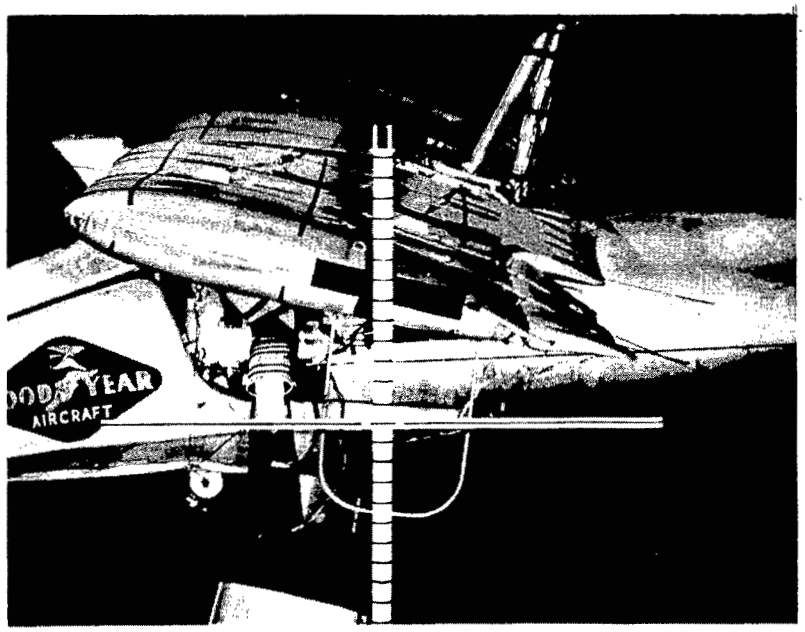

Upper camera; $\alpha = -3.1^{\circ}$; L = 904 lb.

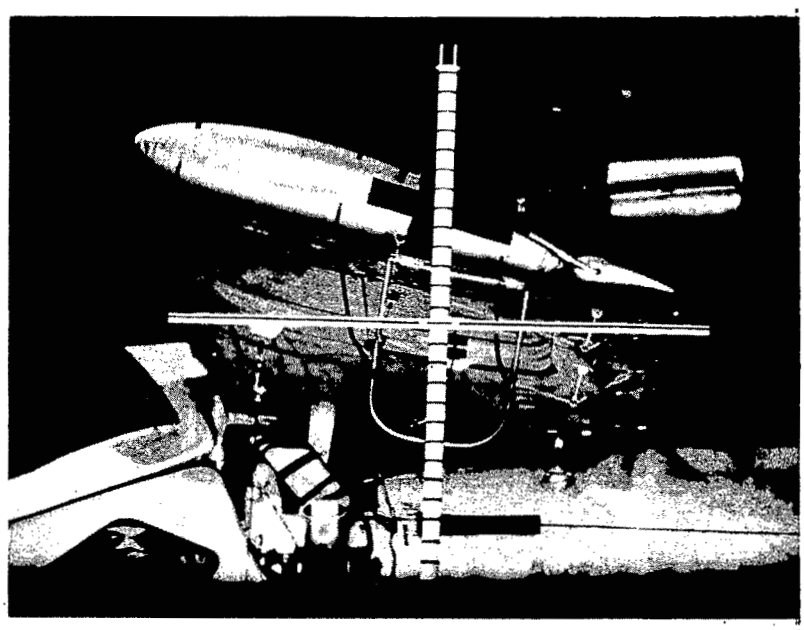

Lower camera; $\alpha = -3.1^{\circ}$; L = 904 lb. L-58-1640

Figure 11.- Concluded.

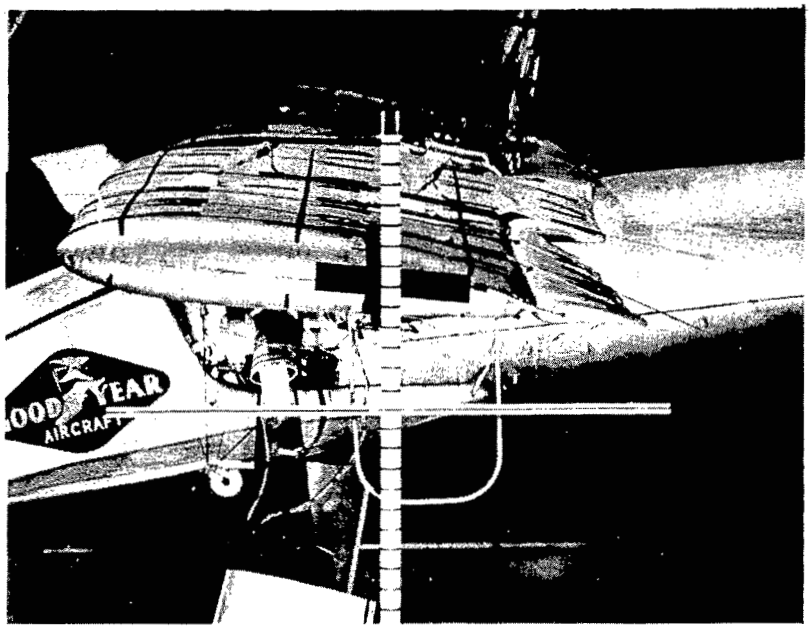

Upper camera; $\alpha = -6.8^{\circ}$; L = 616 lb.

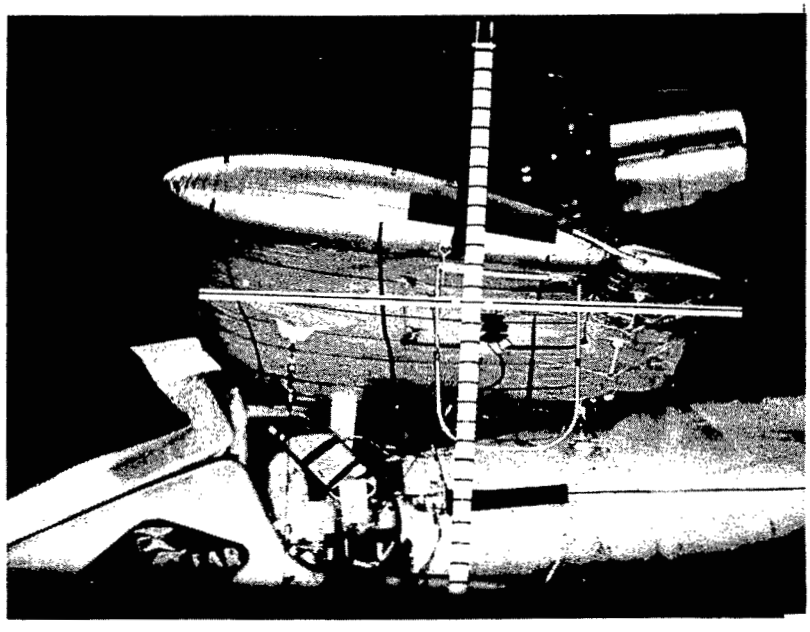

Lower camera; $\alpha = -6.8^{\circ}$; L = 616 lb. L-58-1641

Figure 12.- Deflection study photographs for original configuration. V = 71 mph; q_{av} = 12.2 lb/sq ft.

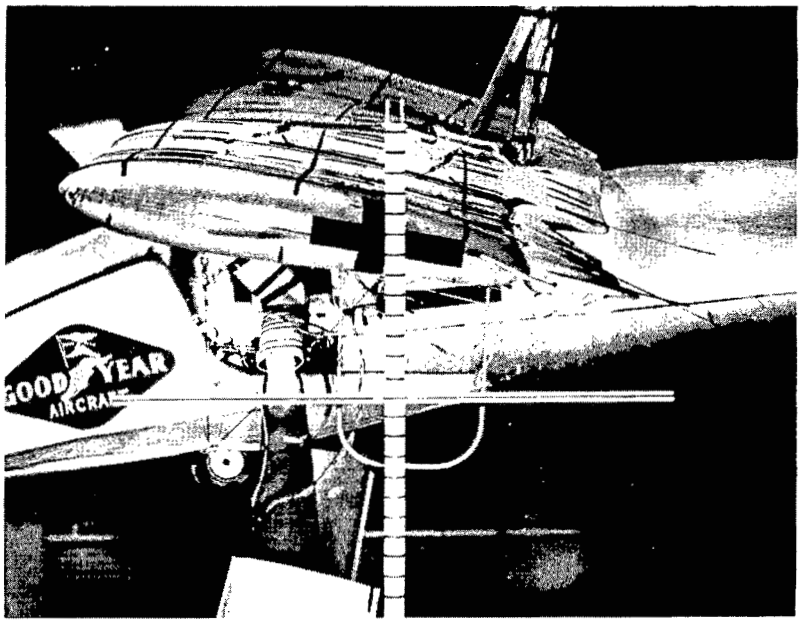

Upper camera; $\alpha = -6^{\circ}$; L = 850 lb.

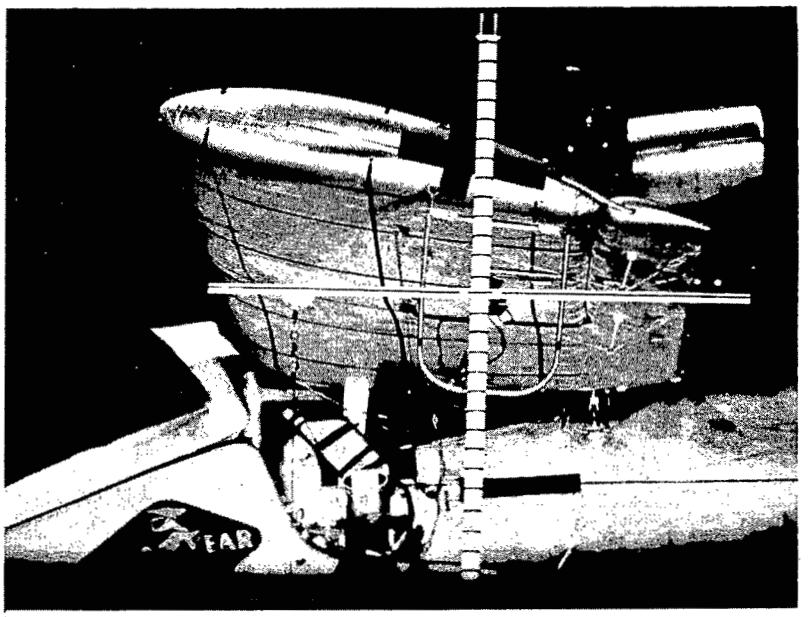

Lower camera; $\alpha = -6^{\circ}$; L = 850 lb. L-58-1642

Figure 12.- Continued.

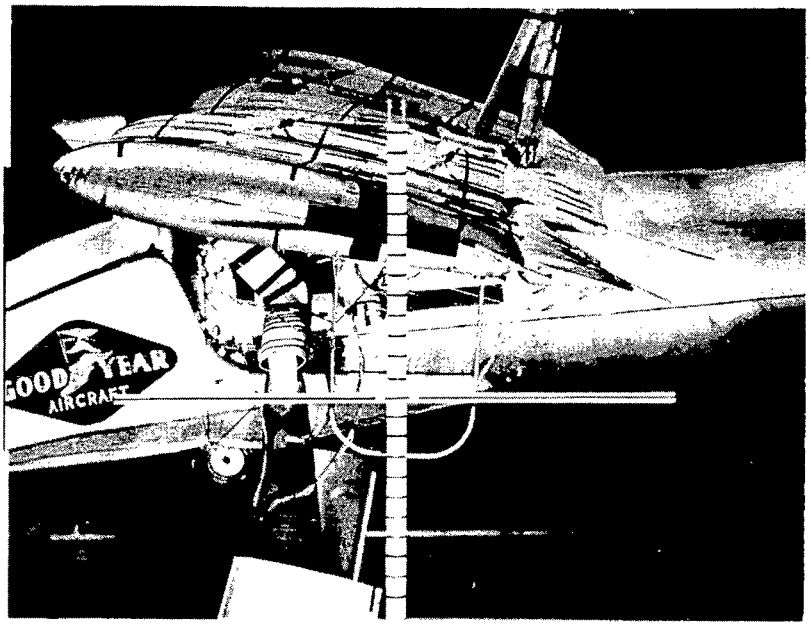

Upper camera; $\alpha = -5.75^{\circ}$; L = 890 lb.

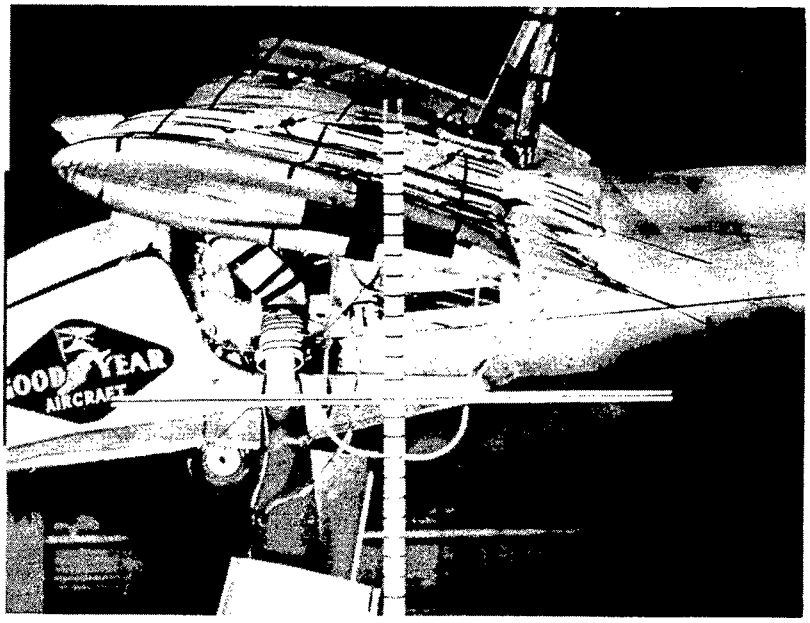

Upper camera; $\alpha = -5.50^{\circ}$; L = 958 lb. L-58-1643

Figure 12.- Continued.

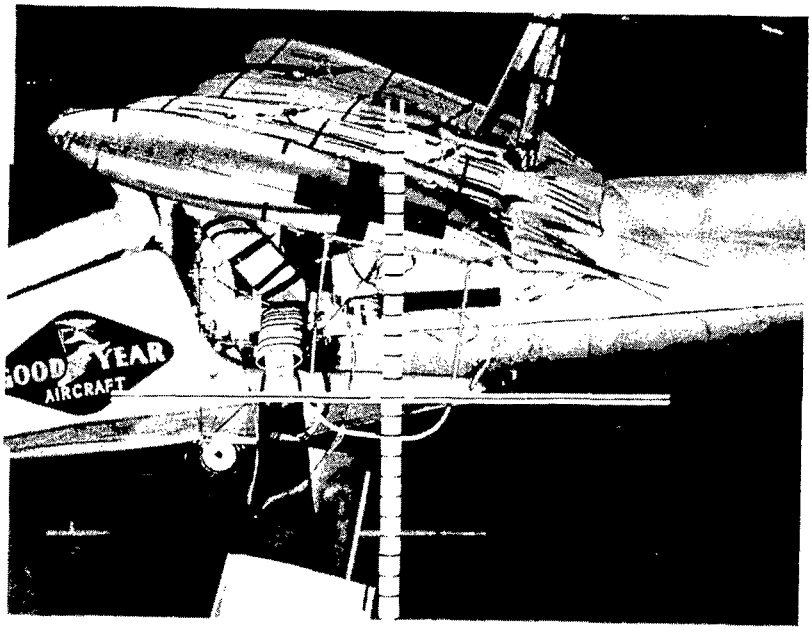

Upper camera; $\alpha = -5.35^{\circ}$; L = 1,011 lb.

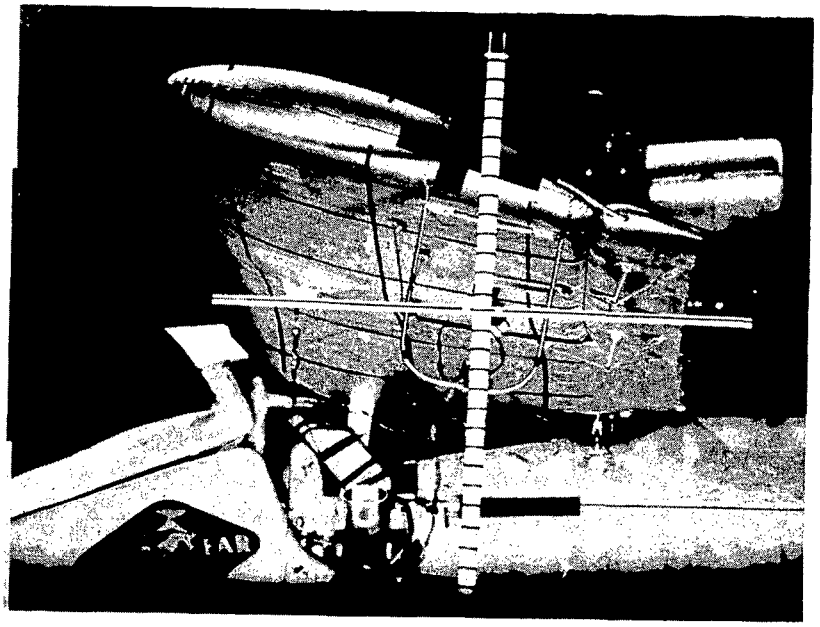

Lower camera; $\alpha = -5.1^{\circ}$; L = 1,100 lb. L-58-1644

Figure 12.- Continued.

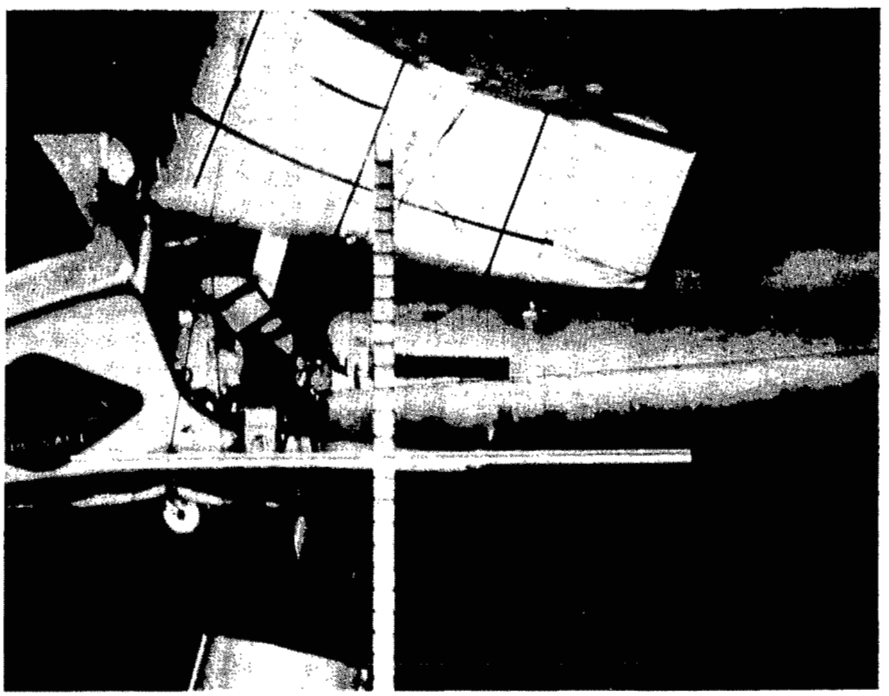

Upper camera; $\alpha = -4.75^{\circ}$. L-58-1645

Figure 12.- Concluded.

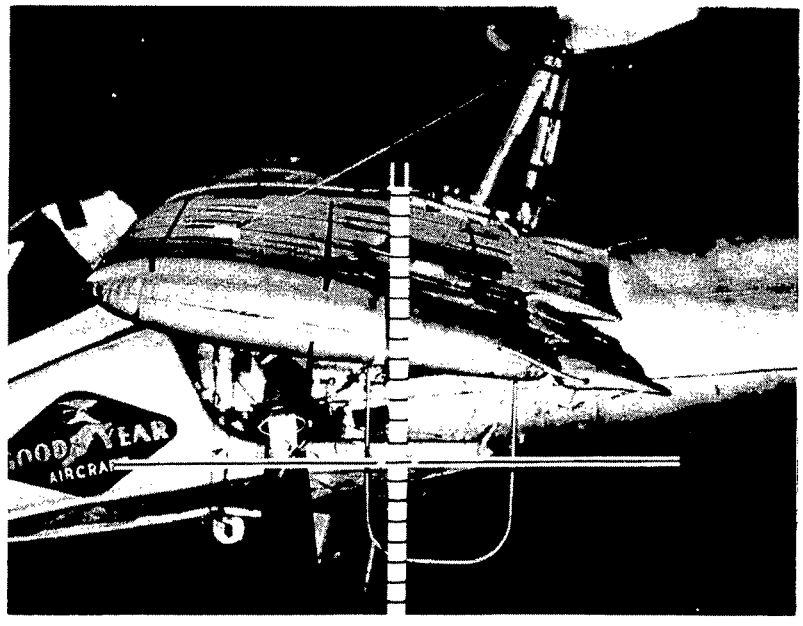

Upper camera; $\alpha = -4.9^{\circ}$; L = 650 lb.

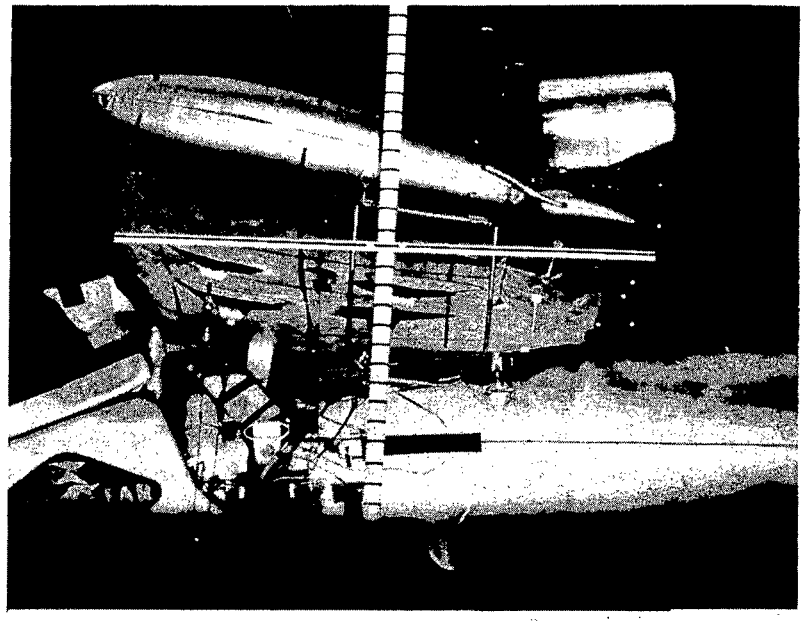

Lower camera; $\alpha = -4.9^{\circ}$; L = 650 lb. L-58-1646

Figure 13.- Deflection study photographs with additional wing guy cables installed. V = 64 mph; q_{av} = 10.15 lb/sq ft.

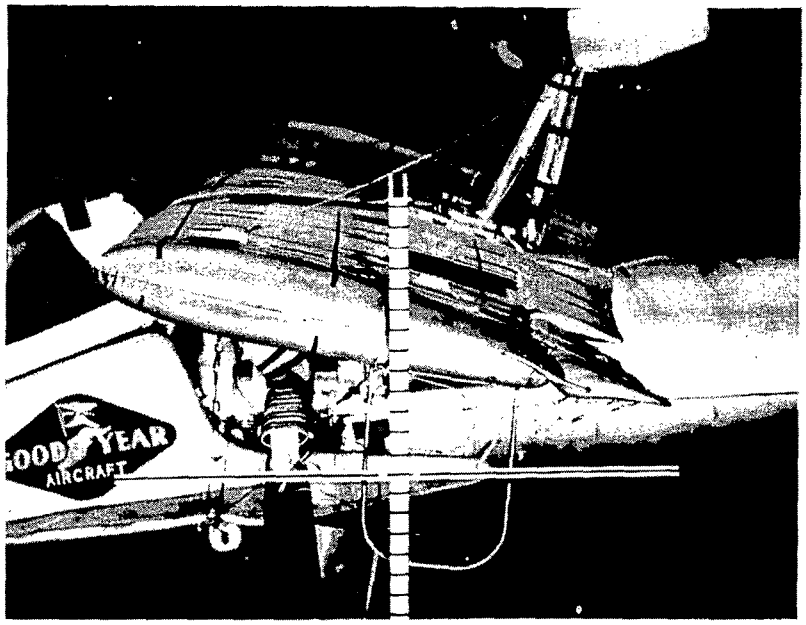

Upper camera; $\alpha = -3.1^{\circ}$; L = 849 lb.

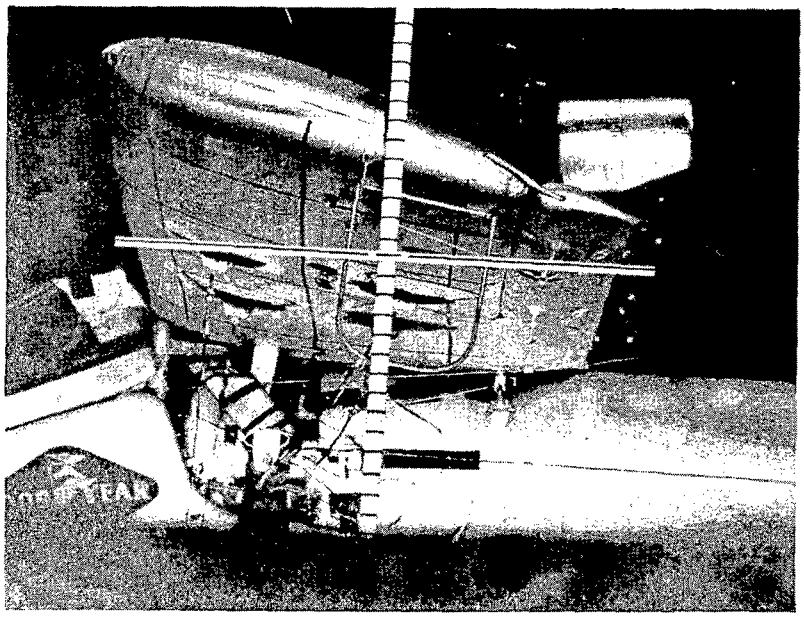

Lower camera; $\alpha = -3.1^{\circ}$; L = 849 lb. L-58-1647

Figure 13.- Continued.

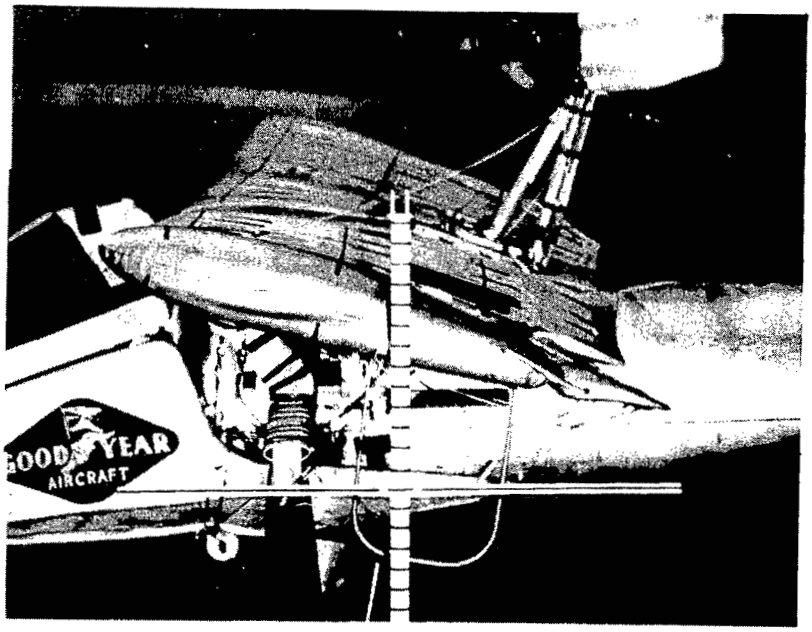

Upper camera; $\alpha = -2.2^{\circ}$; L = 971 lb.

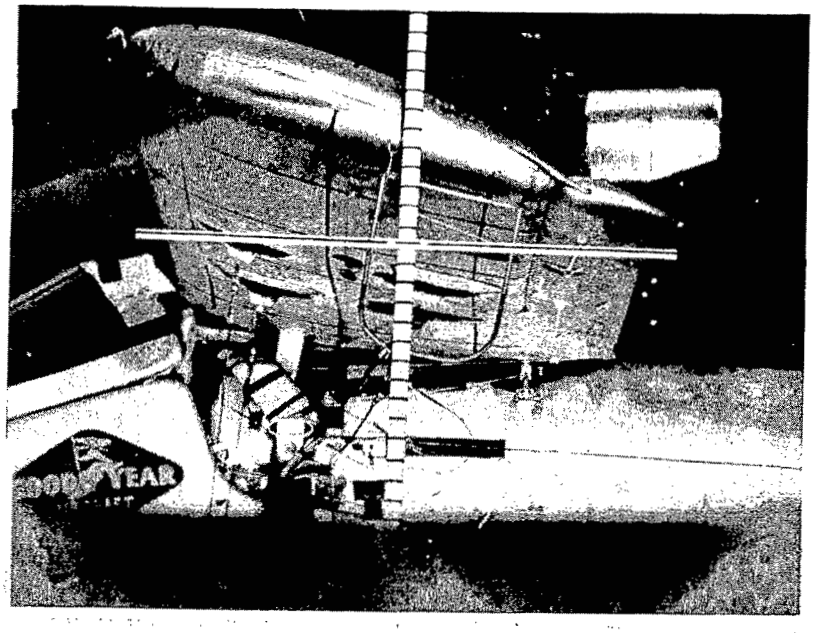

Lower camera; $\alpha = -2.2^{\circ}$; L = 971 lb. L-58-1648

Figure 13.- Continued.

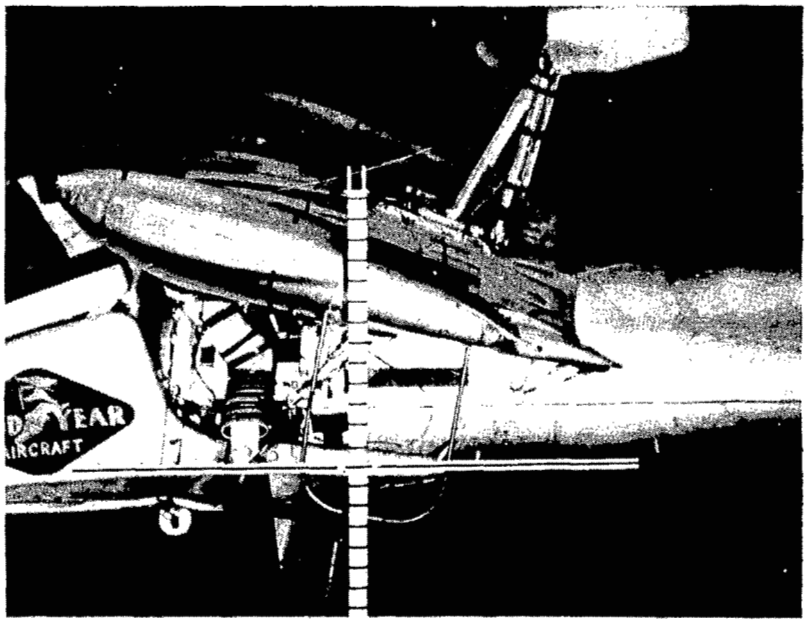

Upper camera; $\alpha = -1.2^{\circ}$; L = 1,086 lb.

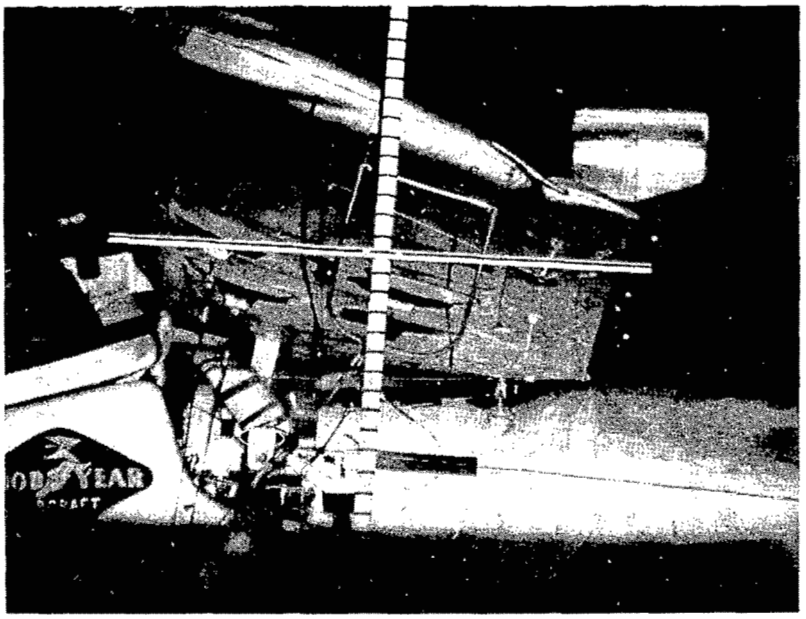

Lower camera; $\alpha = -1.2^{\circ}$; L = 1,086 lb. L-58-1649

Figure 13.- Continued.

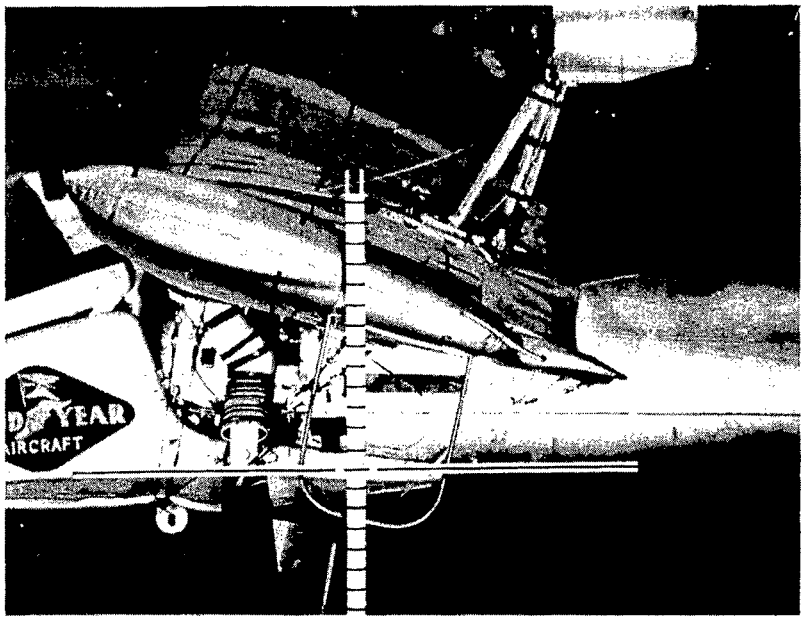

Upper camera; $\alpha = -0.3^{\circ}$; L = 1,126 lb.

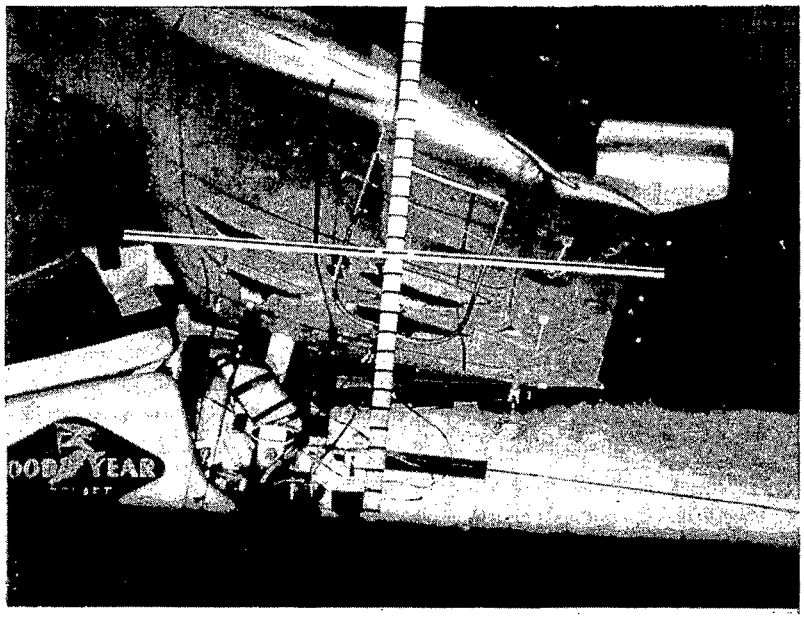

Lower camera; $\alpha = -0.3^{\circ}$; L = 1,126 lb. L-58-1650

Figure 13.- Concluded.

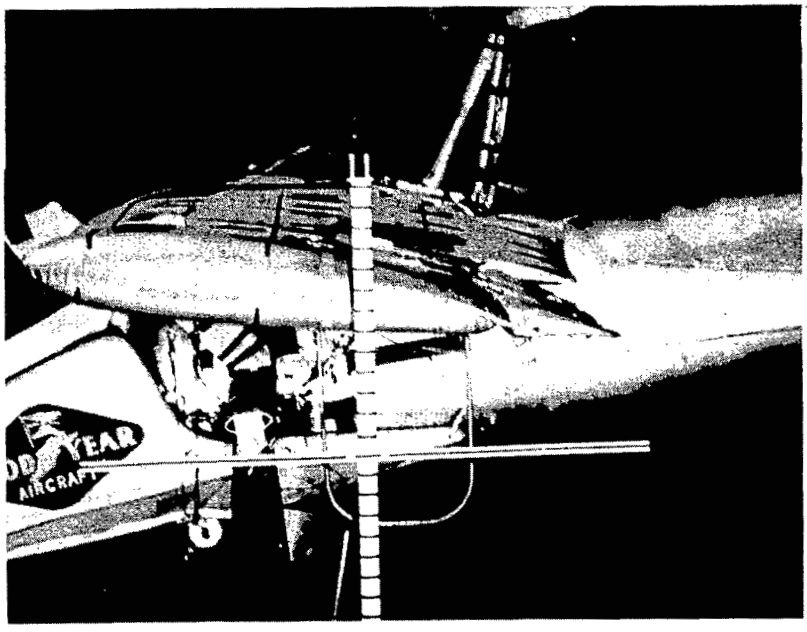

Upper camera; $\alpha = -6.8^{\circ}$; L = 554 lb..

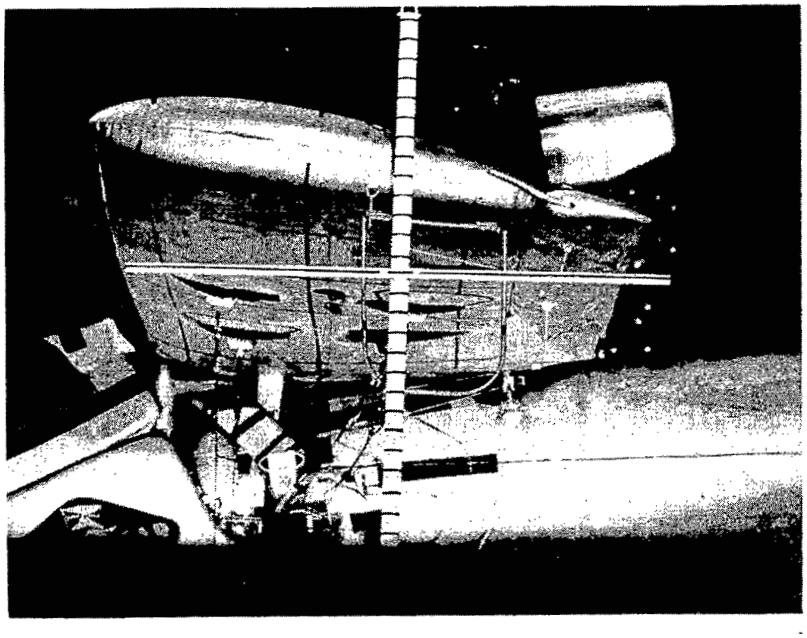

Lower camera; $\alpha = -6.8^{\circ}$; L = 554 lb. L-58-1651

Figure 14.- Deflection study photographs with additional wing guy cables installed. V = 71 mph; q_{av} = 12.4 lb/sq ft.

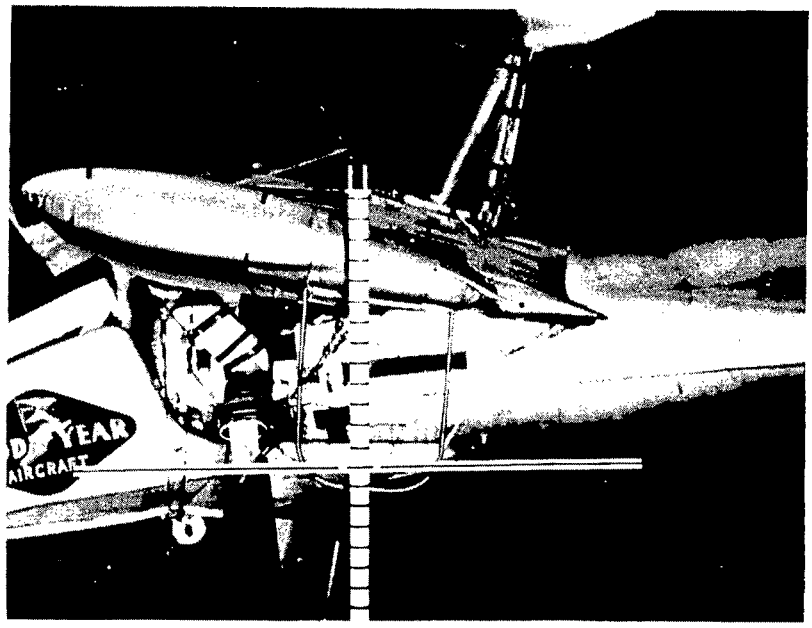

Upper camera; $\alpha = -4.9^{\circ}$; L = 889 lb.

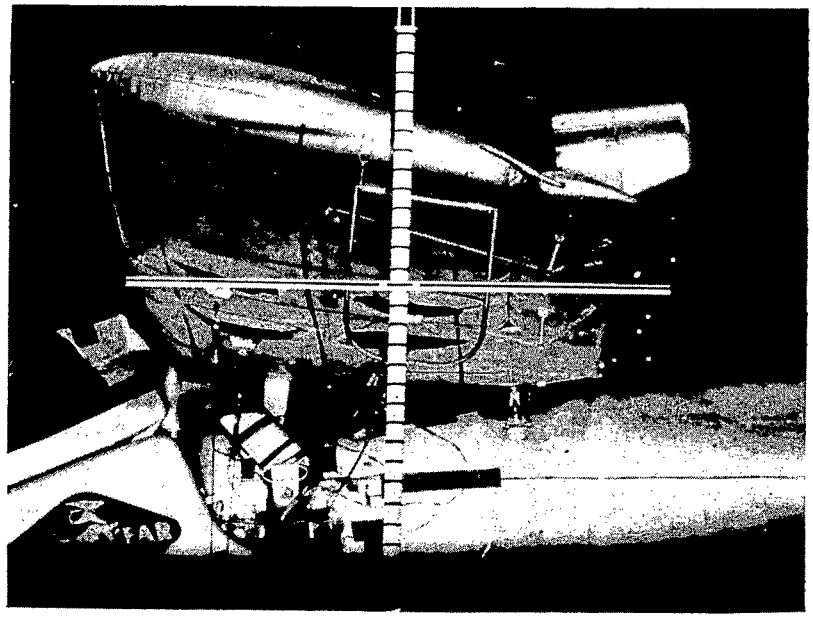

Lower camera; $\alpha = -4.9^{\circ}$; L = 889 lb. L-58-1652

Figure 14.- Continued.

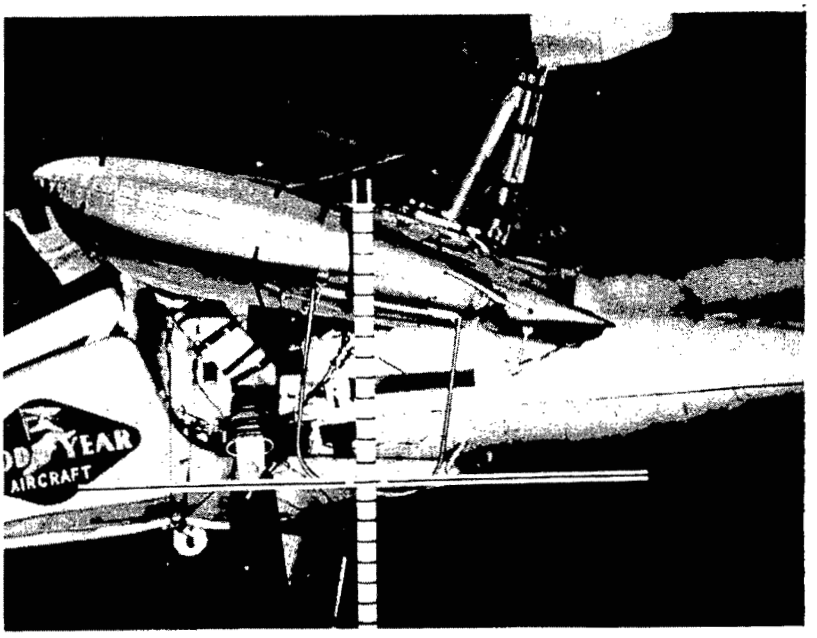

Upper camera; $\alpha = -4.1^{\circ}$; L = 1,089 lb.

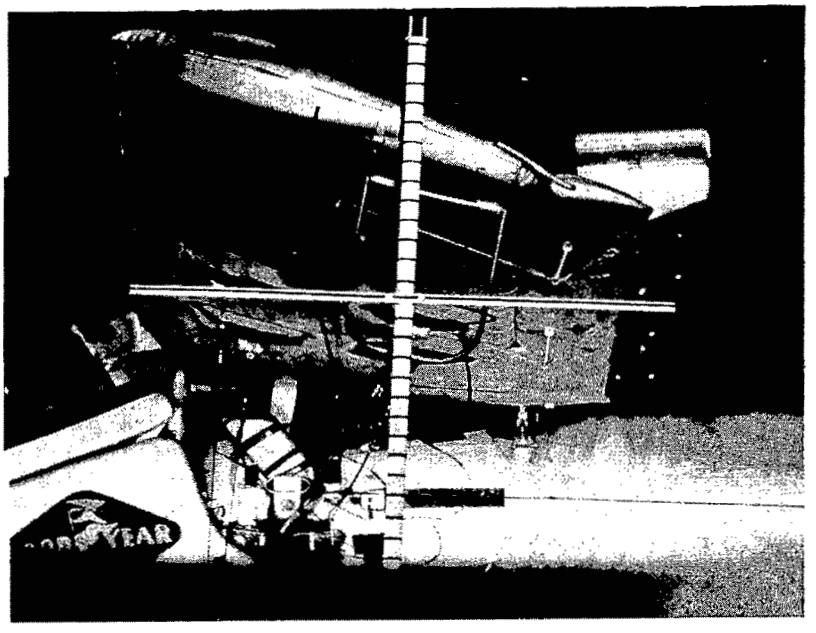

Lower camera; $\alpha = -4.1^{\circ}$; L = 1,089 lb. L-58-1653

Figure 14.- Continued.

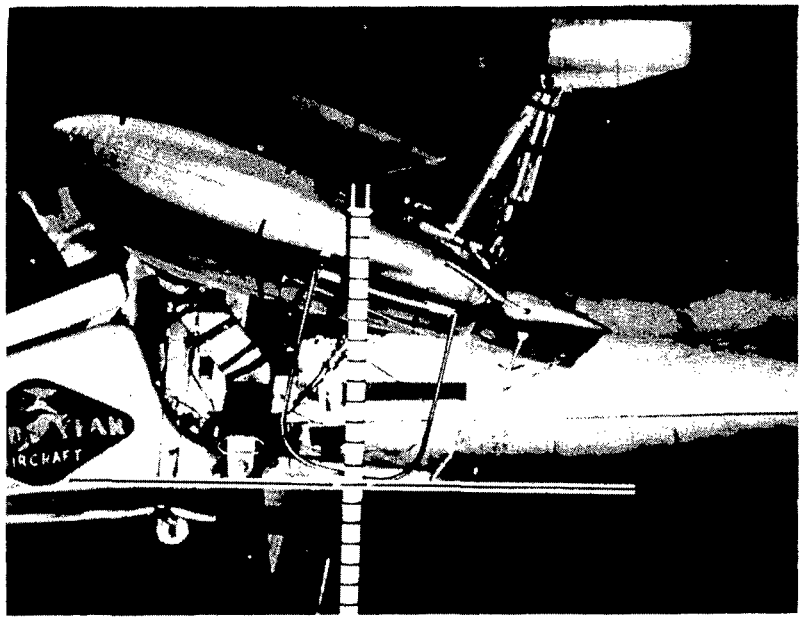

Upper camera; $\alpha = -3.2^{\circ}$; L = 1,300 lb.

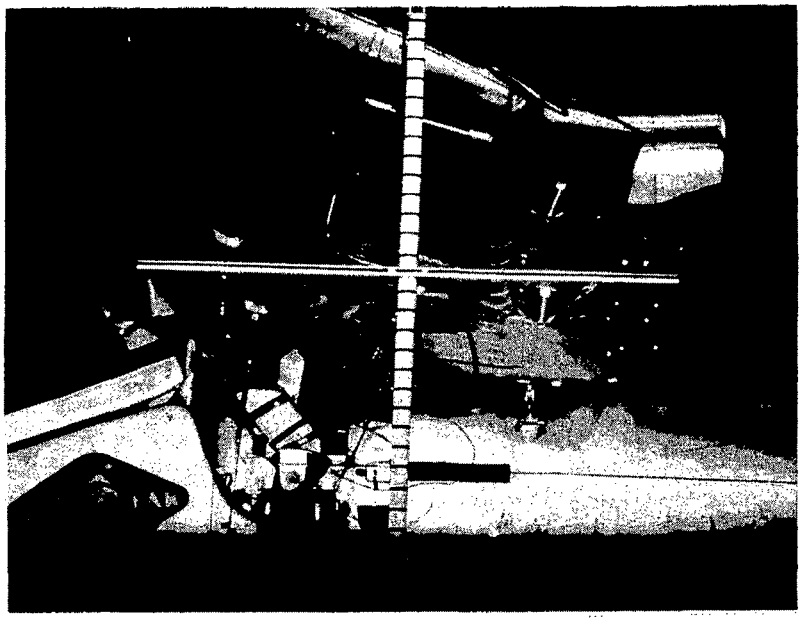

Lower camera; $\alpha = -3.2^{\circ}$; L = 1,300 lb. L-58-1654

Figure 14.- Continued.

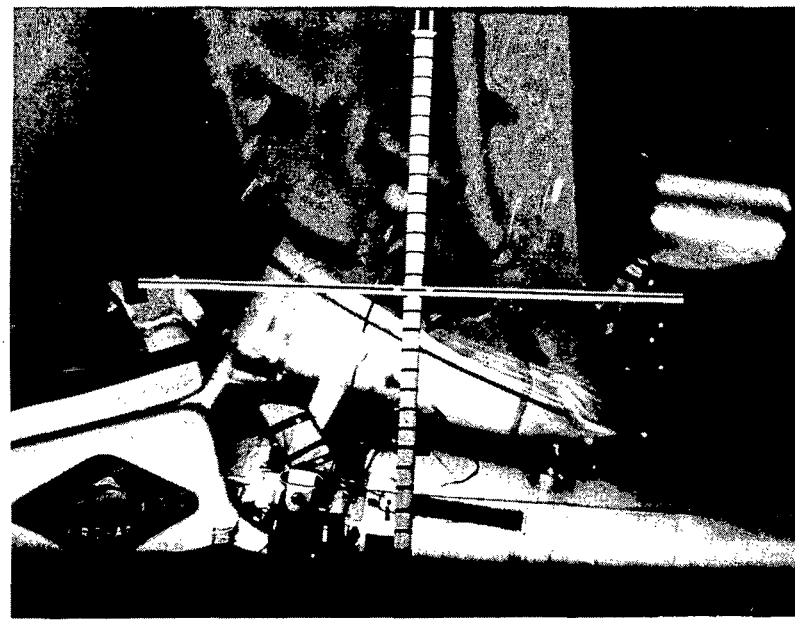

Lower camera; $\alpha = -3^{\circ}$.

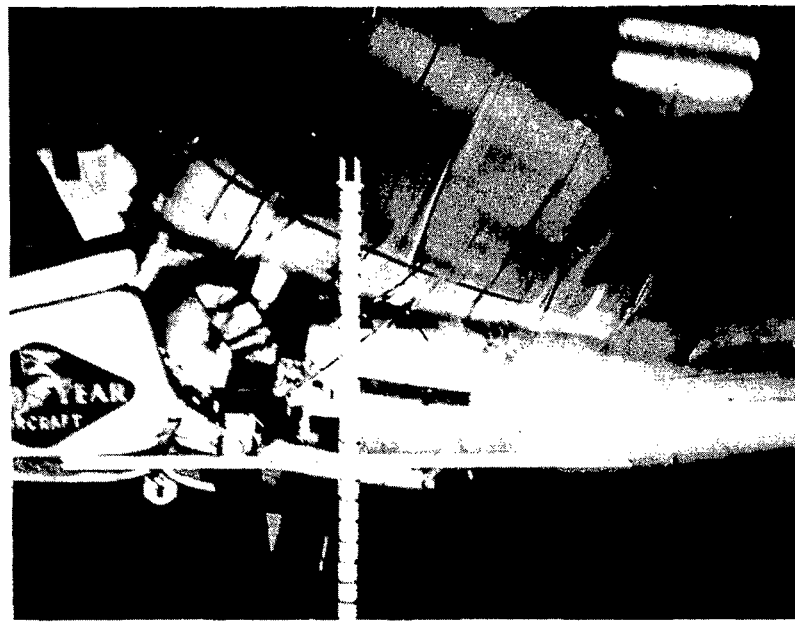

Upper camera; $\alpha = -3^{\circ}$. L-58-1655

Figure 14.- Concluded.

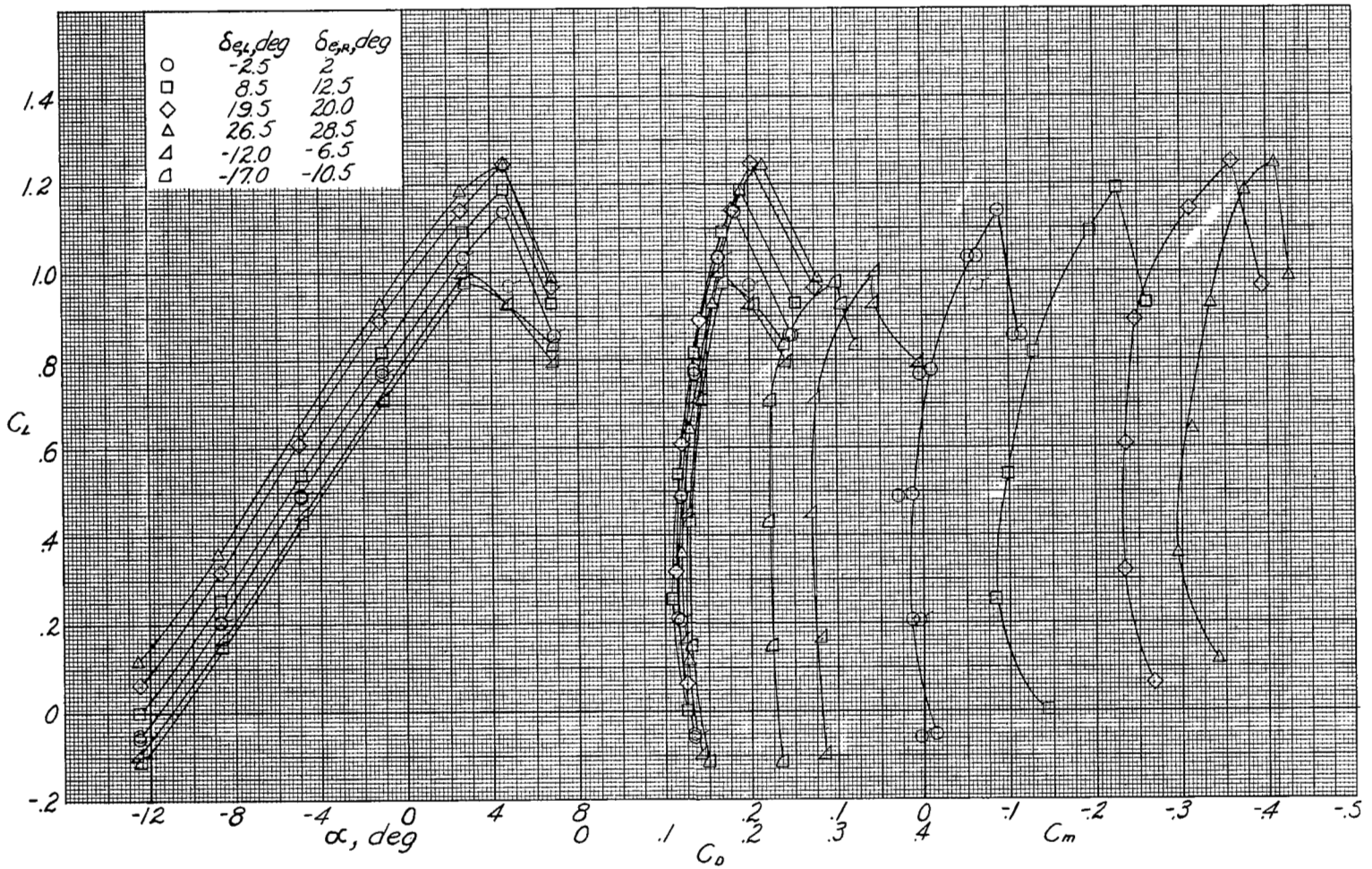

(a) Wind velocity, 41 mph; q_{av} = 4 lb/sq ft.

Figure 15.- Effect of elevator deflection on aerodynamic characteristics of the Goodyear Inflatoplane. Original configuration; normal inflation pressure (7 lb/sq in.); canopy installed.

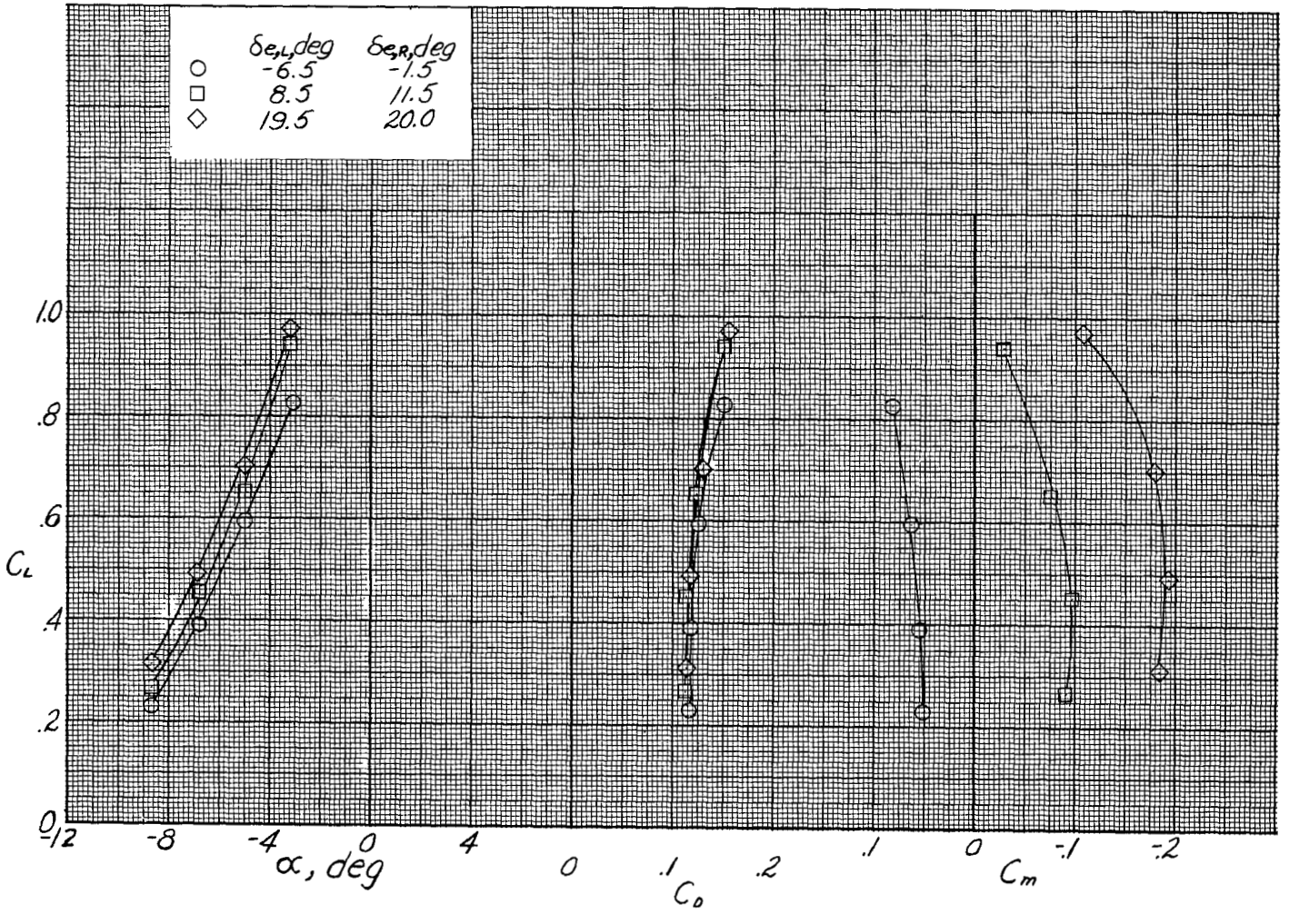

(b) Wind velocity, 64 mph; q_{av} = 10.

Figure 15.- Concluded.

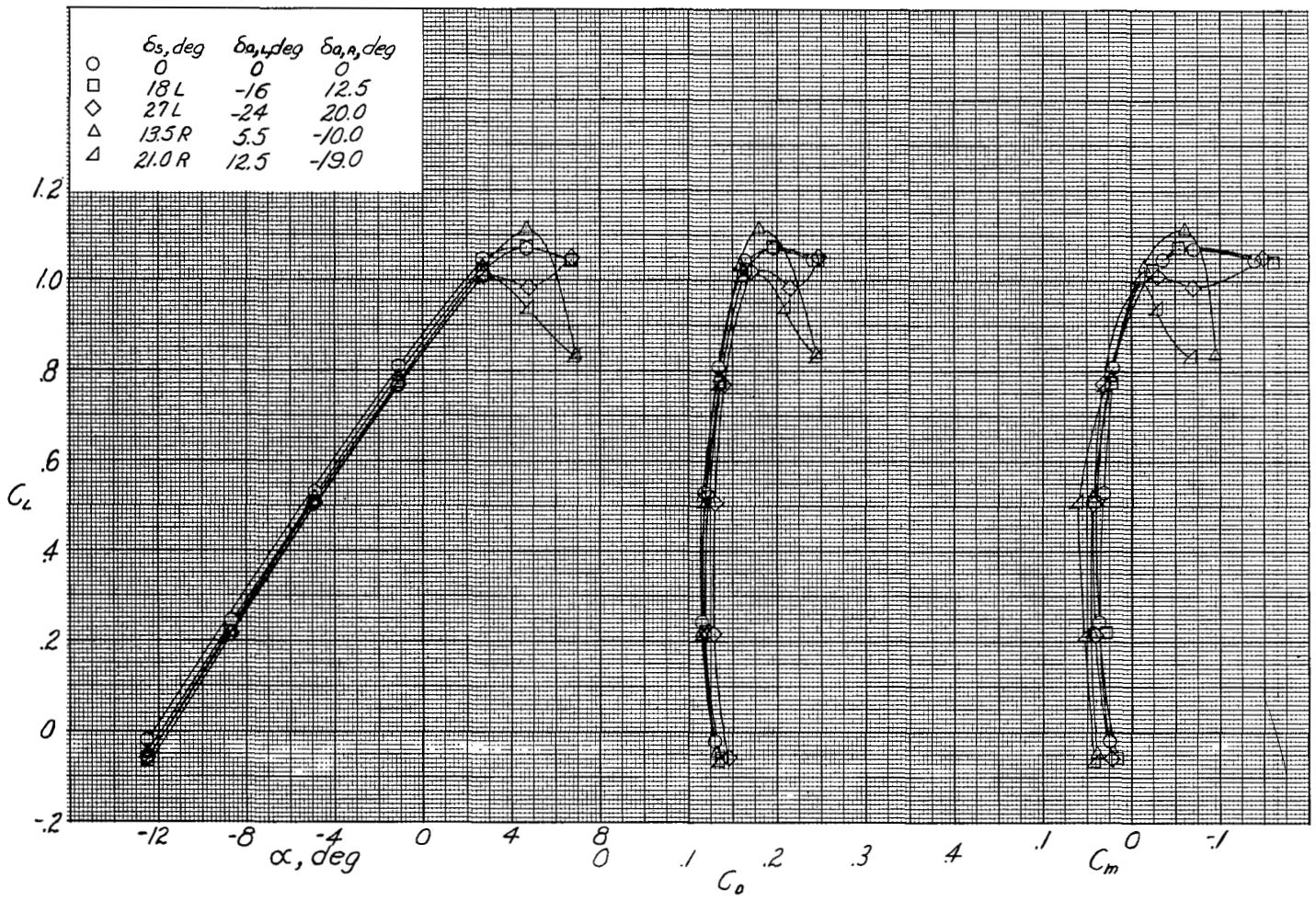

Figure 16.- Effect of aileron deflection on aerodynamic characteristics of the Goodyear Inflatoplane. Original configuration; normal inflation pressure (7 lb/sq in.); canopy installed; wind velocity approximately 41 mph (q_{av} = 4 lb/sq ft).

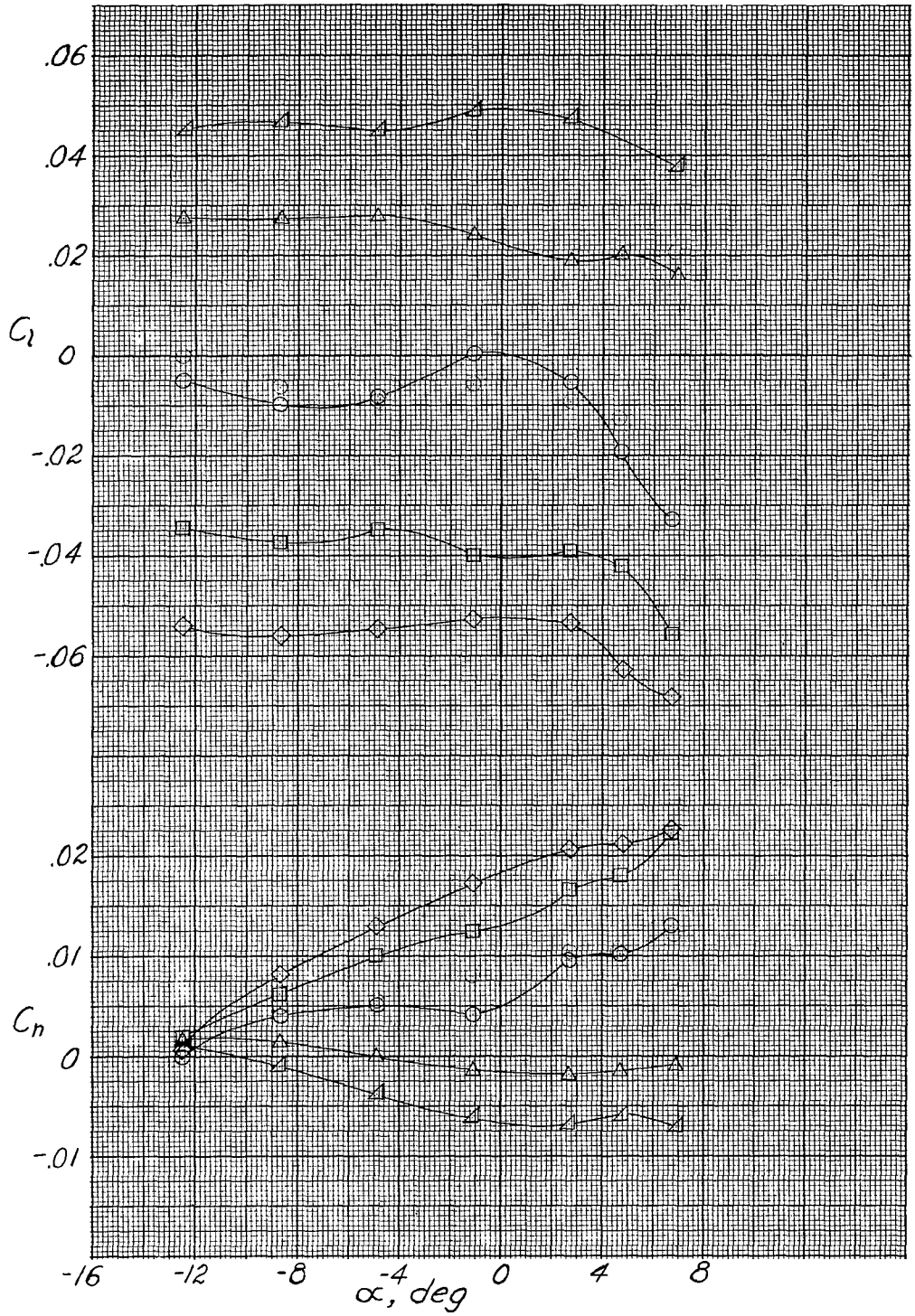

Figure 16.- Concluded.

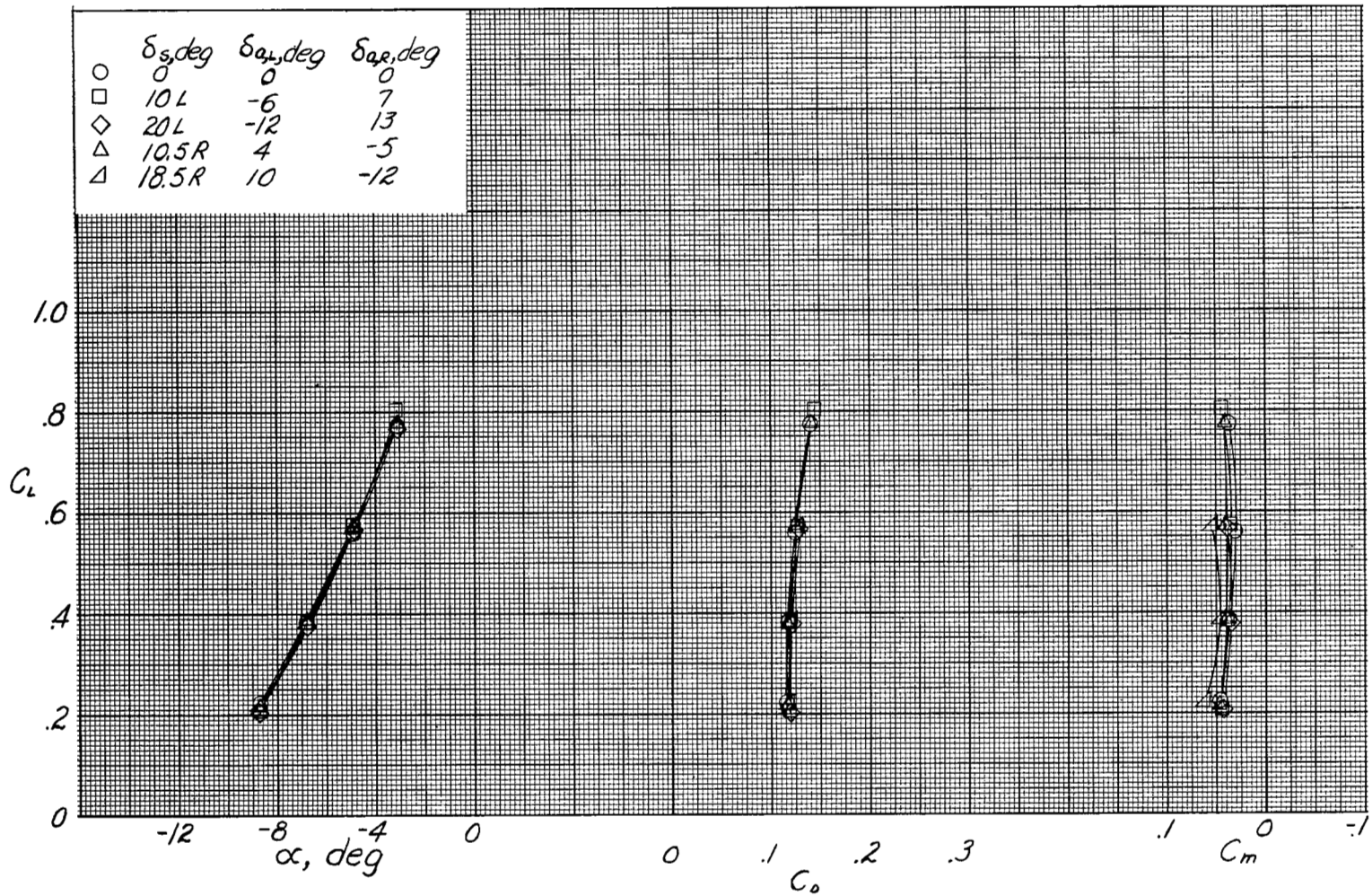

Figure 17.- Effect of aileron deflection on aerodynamic characteristics. Original configuration; normal inflation pressure (7 lb/sq in.); canopy installed; wind velocity approximately 64 mph $\left(q_{av} = 10 \text{ lb/sq ft}\right)$.

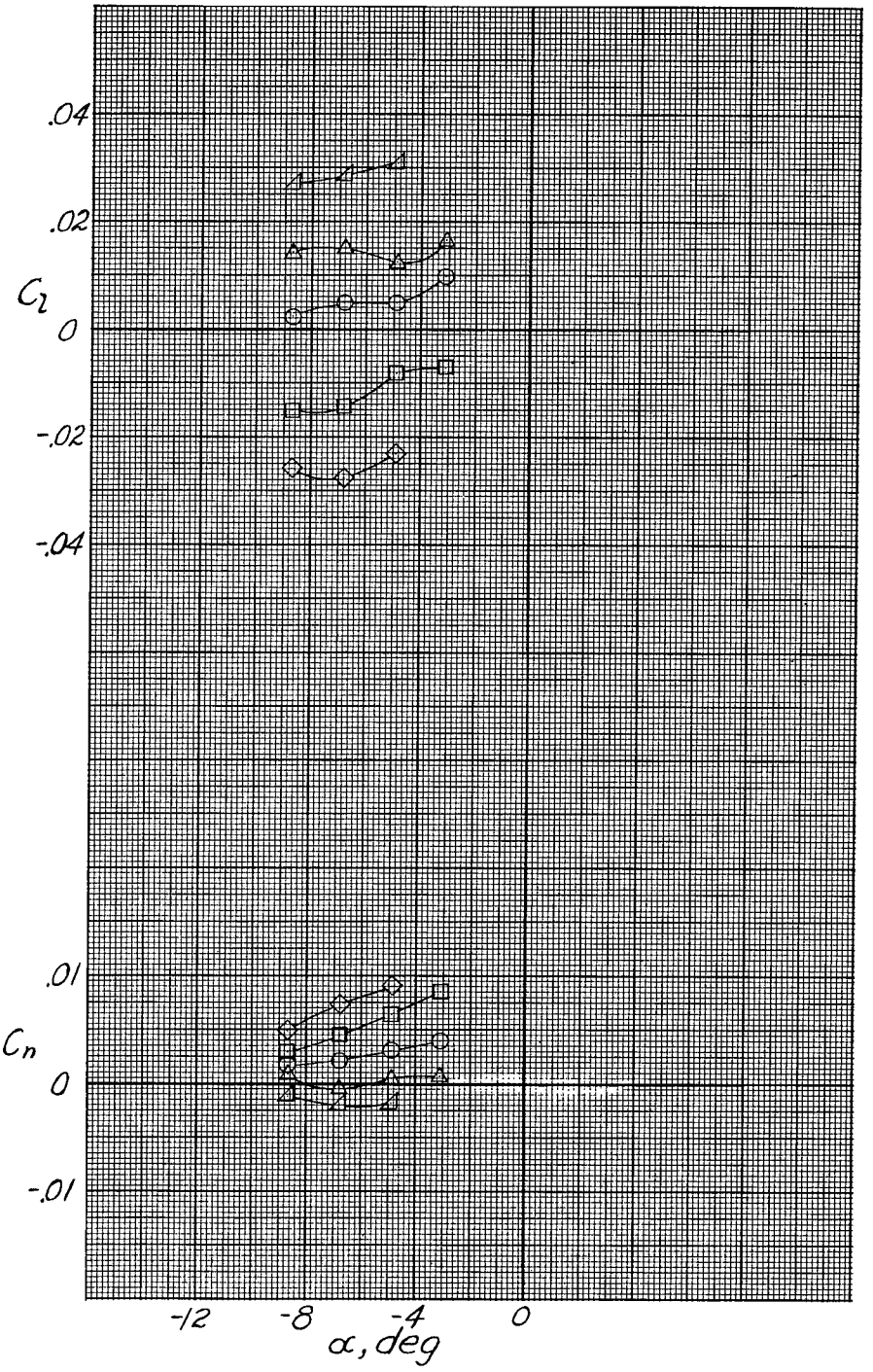

Figure 17.- Concluded.